Electrical Power and Energy Systems 158 (2024) 109916

Contents lists available at ScienceDirect

International Journal of Electrical Power and Energy Systems

journal homepage: www.elsevier.com/locate/ijepes

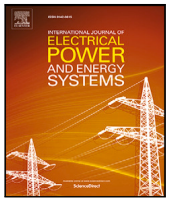

Tri-level scheduling of integrated electric vehicle parking lots and solar distributed generations in local and wholesale electricity markets

Saeed Zeynali [a], Nima Nasiri [b], Sajad Najafi Ravadanegh [b,*], Sylvain Kubler [a], Yves Le Traon [a]

[a] SnT, University of Luxembourg, 6 Rue Richard Coudenhove-Kalergi, L-1359 Luxembourg, Luxembourg
[b] Resilient Smart Grids Research Lab, Electrical Engineering Department, Azarbaijan Shahid Madani University, Tabriz, Iran

ARTICLE INFO

Keywords:
Alternating direction method of multipliers
Electric vehicles
Local electricity market
Robust optimization
Stochastic programming
Wholesale electricity market

ABSTRACT

This study investigates a tri-level optimal market strategy for the integrated electric vehicle fleets and solar distributed generations (IEVSDG) to engage in the local electricity market (LEM) as a strategic price-maker. The distribution company (Disco) which operates the LEM, participates in the wholesale electricity market (WEM) to provide its consumers, is also a strategic price-maker. For this purpose, the IEVSDGs are integrated at the first level of the optimization problem, while the Disco operator and WEM operator form the second and third levels, respectively. In other words, Disco acts as an intermediary retailer that links the LEM (modelled by IEEE 69-bus distribution system) to WEM (modelled by an IEEE 24-bus transmission network). The study puts forward a novel solution strategy, where the second and third level problems are conjoined through the Karush–Kuhn–Tucker (KKT) conditions. Moreover, the equilibrium point between the first level and this conjoined problem is achieved through the alternating direction method of multipliers (ADMM). In a hybrid robust optimization (RO) and stochastic programming (SP) approach, the uncertain specifications, such as the arrival/departure times and daily travelled miles are modelled through the SP scenarios. On other hand, the RO was deployed to handle solar power forecasting uncertainties. Different case studies of dumb and smart charging were devised to evaluate the method. The outcomes show that the proposed three-level approach leads to 57.21% reduction in the LEM price, and 0.86% reduction in the WEM price. Furthermore, the smart charging strategy eliminated 105 MWh of load interruptions.

1. Introduction

1.1. Background

The widespread adoption of distributed generation (DG) units has undeniably transformed electric distribution systems, turning them from passive consumers bound by market prices into active participants with control over their energy demand [1]. Accordingly, with the integration of DGs, the distribution system earned a new title as an active distribution system (ADS) since it was enabled to supply active energy and be part of the production chain [2]. Another imperative breakthrough in electricity distribution was marked by the liberalization of the electricity markets that laid the foundation of the modern and free marketplace. In turn, this phenomenon led to substantial improvements in both quality and efficiency of the production and distribution [3].

At a global level, the transportation sector attributes the highest energy consumption by accounting for 29% of the global energy demand [4]. As a result, it has been designated as one of the main polluters by accounting for 7 billion tons of the global CO2 emissions [5]. Moreover, some studies estimate that transportation sector takes up 65% of the global oil consumption [6]. The increasing awareness about the climate change has forced this problem on highest propriety of the global agenda. In this concern, transportation electrification has been unanimously designated as a feasible solution. For instance, the UK has enforced legislation to halt the sales of the petroleum-based vehicles by 2030, while simultaneously setting up goals to achieve a zero-emission energy sector [7]. The latest research indicate that in 2022 up to 40% of the UK's energy was supplied through renewable energy forms, which is targeted to reach net zero value by 2035 [8].

The sharp ongoing increase in the penetration level of electric vehicles (EV) has created deep concerns around their impact on the power systems' security. In this regard, the consensus is that their coordinated charging is the key for addressing peak-shaving requirements and secure operation [9]. On the other hand, solar distributed generations (SDGs) have shown a dramatic decline in production cost, which has made them a popular green energy form, and they are currently increasingly deployed in urban centres. Considering the high penetration of these SDGs and idle EVs at smart parking lots, their

* Corresponding author.
E-mail address: s.najafi@azaruniv.ac.ir (S.N. Ravadanegh).

https://doi.org/10.1016/j.ijepes.2024.109916
Received 18 April 2023; Received in revised form 3 February 2024; Accepted 3 March 2024
Available online 11 March 2024

Nomenclature

Abbreviations

IEVSDG	Integrated electric vehicle fleets and solar distributed generations
LEM	Local electricity market
Disco	Distribution company
WEM	Wholesale electricity market
KKT	Karush–Kuhn–Tucker
ADMM	alternating direction method of multipliers
RO	Robust optimization
SP	Stochastic programming
DG	Distributed generation
ADN	Active distribution system
TN	Transmission network
Genco	Generation company
EV	Electricity vehicle
EVF	Electricity vehicle fleet
MCP	Market clearing price

Sets and indices

s, t	Index of time, scenario
v, kl	Index of IEVSDG, linearization segments
k, l, d	Index of DG, interruptible loads, demand
i, j	Index of ADN nodes
b,b′, g	Index of TN nodes, Genco
m	Index of generation blocks
A_y^x	Set of connectivity between x and y

Parameters

ρ	penalty factor
π_s	Probability of each scenario
$\lambda_{t,i}^{LEM*}$	Optimal value of MCP of LEM ($/MW)
c_v^{pv}	Operation cost of SDGs ($/MW)
η_v, EB_v	The efficiency/capacity of the EVF battery (MWh)
$TA_{s,v}$, $TD_{v,s}$	Arrival/departure time of EVF
$SOC_{v,s}^{In}$, SOC_v^{des}	Initial/Desired SOC of the EVFs
$\underline{SOC_v}$, $\overline{SOC_v}$	Min/Max SOC of EVFs
$\overline{SOC_{v,s}^{end}}$	SOC of EVFs at departure
$DT_{v,s}$	Driven miles by EVFs (mile)
EM_v	Energy consumption per mile (MWh/mile)
Cr	Nominal charging rate of EVFs (MW)
a_0	Degradation function fitting parameter
BC_v	Battery cost of EVFs ($)
$\overline{p_{v,t}^{pv}}$, $\hat{p}_{v,s,t}^{pv}$	Maximum/Deviation of SDG power (MW)
Γ^{RO}	The robustness budget of RO
C_l^{IL}, C_k^{DG}	Cost of interruptible loads,DGs ($/MWh)
$C_{g,m}^{G}$	Cost of linear DG generation block ($/MWh)
$\underline{p_k^{DG}}$, $\overline{p_k^{DG}}$	Min/Max DG power (MW)
$\widehat{C_k^S}$, $\widetilde{C_k^S}$	Start-up/shutdown cost of DG ($)
$\widehat{R}_k$, $\widetilde{R}_k$	Ramp up/down rate of DG (MW)
T_k^{Ue}, T_k^{De}	Minimum up/down time of DG (h)
RU_g, RD_g	Ramp up/down rate of Genco (MW)
T_k^{U0}, T_k^{D0}	Minimum up/down time at the beginning (h)
R_{ij}^{DS}, Z_{ij}^{DS}	Resistance/Impedance of feeders (Ω)
$\overline{I_{ij}^{DS}}$	Maximum ADS current (KA)
$\underline{V_i^{DS}}$, $\overline{V_i^{DS}}$	Min/Max ADS voltage (kV)
$\overline{C_{b,b'}^{Max}}$	Maximum capacity of TN lines (MW)
$P_{d,t}^{DSL}$	ADS load (MW)
$B_{b,b'}$	Susceptance of TN feeders ($1/\Omega$)
$P_{d,t}$	Genco demand (MW)
$\underline{p_t^{Dsc}}$, $\overline{p_t^{Dsc}}$	Min/Max power exchange of ADS with WEM (MW)

Variables

OF_1, OF_2, OF_3	First, second, and third level objectives ($)
$p_{v,s,t}^{+}$, $p_{v,s,t}^{-}$	Charging/Discharging power of EVFs (MW)
$p_{v,s,t}^{pv}$	The power dispatched from SDGs (MW)
$dg_{v,s,t}^{Lin}$, $dg_{v,s,t}^{Nl}$	Linear/nonlinear battery erosion cost ($)
$SOC_{v,s,t}$	State of charge of EVFs.
C_t^{Dsc}	Offer price of Disco
$\overline{P}_g$	Maximum power generation of Genco (MW)
$\sigma_{v,s,t}$	Cycle depth of EVFs
$\psi_{v,s,t}$	Cycle depth degradation of EVFs
$MD_{v,s,t}$	Marginal battery degradation ($/MW)
$\vec{P}_{t,v}^{ES}$, $\overleftarrow{P}_{t,v}^{ES}$	The exported/imported IEVSDG power (MW)
$y_{v,s,t}^{aux1}$, $y_{v,s,t}^{aux1}$	Auxiliary variables in degradation linearization
$\hbar_{kl,v,s,t}^{a1}$, $\hbar_{kl,v,s,t}^{a2}$	Semi-integer variable used in degradation linearization.
$FY_{v,s,t}^{aux1}$, $FY_{v,s,t}^{aux2}$	Linear decompositions of the degradation cost function.
$\lambda_{b,t}^{WEM}$, $\lambda_{t,i}^{LEM}$	The MCP of WEM/LEM ($/MWh)
p_t^{Dsc}	The power exchange of Disco with WEM (MW)
$p_{l,t}^{IL}$, $P_{k,t}^{DG}$	Interruptible load, DG power (MW)
$\widehat{S}_{k,t}$, $\widetilde{S}_{k,t}$	Start-up/shutdown cost of DG ($)
$\overleftrightarrow{P}_{v,t}^{ES}$	Energy exchange of Disco with IEVSDG (MW)
$P_{ij,t}^{flow}$	Power flow from node i to j (MW)
$V_{i,t}^{DS}$, $\widehat{V}_{i,t}^{DS}$	ADS Voltage and linear square of ADS voltage (kV)
$P_{ij,t}^{Loss}$	Feeder power loss (MW)
$I_{ij,t}^{DS}$, $\widehat{I}_{ij}^{DS}$	Feeder current and linear square of it (A)
$\lambda_{t,i}^{LEM}$, $\lambda_{t,i}^{WEM}$	MCP of LEM/WEM ($/MWh)
$\rho_{g,m,t}^{G}$	Maximum power generation block of Genco (MW)
$\delta_{b,t}$	The voltage angle of TN node
$P_{g,t}^{G}$	The Genco generation (MW)

Binary variables

$uc_{v,s,t}$, $ud_{v,s,t}$	Charge/discharge state of EVFs
$I_{k,t}$	Commitment state of DG
$y_{k,t}, z_{k,t}$	Start-up/shutdown state of DG

Dual variables

μ, v, ζ	Inequality dual variable.
$x_{v,s,t}^{RO}$, $z_{v,s,t}^{RO}$, $p_{v,s,t}^{RO}$, $y_{v,s,t}^{RO}$	The dual auxiliary variables of RO

cooperation in form of integrated electric vehicle fleets and solar distributed generations (IEVSDG) would be beneficial for both sides. Accordingly, not only the green solar energy usage will be maximized,

but also the transportation sector will be greener and economical [10]. Furthermore, they can take part in the local electricity market (LEM) to submit offers/bids that can maximize their collective profit as they can exert influence in the local market [11]. That said, the distribution company (Disco), which operates the LEM, procures part of its energy through the wholesale electricity market (WEM) [12].

Therefore, the Disco must submit the best offer/bids in WEM. In fact, there are three levels of operators that must coordinate IEVSDG, Disco and WEM, which requires a multi-level optimization tool to reach the best equilibrium state. Furthermore, the arrival/departure time of EVs and their daily travelled miles, along with the SDG production, are uncertain data that should be accounted for with novel methods [13]. The EV aggregators have gained a great deal of popularity in recent publications [14]. The reason is that a single EV cannot participate in the energy markets and have a significant influence on the power system comparable to a drop in the ocean. Admittedly, it can improve the profits of the owner by following the price/load patterns as a price-taker. Nevertheless, when aggregated at great numbers, EVs could engage in the electricity markets and improve the collective profit of the owners by their market strategies as a price-maker rather than a price-taker that has no authority over the market-clearing price (MCP) [15].

1.2. Literature review

The vehicle to grid capabilities of an idle EV was effectively utilized by [16] to enhance home energy management strategies in the form of demand response and interruptible loads (IL) for emergency purposes. In [17], the charging stations were assigned to the EVs considering vacancy positions. Afterward, the optimal scheduling was conducted via the 2-PEM method considering the EVs demand as an uncertain parameter. The congestion issue will be a serious threat to the well-being of the distribution system. In this respect, Ref. [18] investigated a congestion-oriented distributed marginal pricing method to control EVs with price signals under the command of an aggregator. The proposed model was a bi-level problem, wherein the aggregator was the upper-level leader, while the disco was the follower. Similarly, the authors in [19] studied the impact of congestion that might be caused by uncoordinated charging. Additionally, the study proposed an analytical strategy to find the highest possible EV penetration level that can be held without line congestion.

In [20], the EVs were modelled as flexible demand response providers in community-integrated energy systems, while multi-stakeholder scenarios were considered through bi-level optimization. A novel exact algorithm was proposed in [21] for EV aggregators to submit offers/bids at the leading stage, while the EV owners were modelled as lower-level followers that self-schedule according to the offer/bid of the aggregator. Furthermore, a distributionally robust stochastic optimization framework was proposed in [22] for collaborative bidding scheduling of wind farms, EV aggregators, and hydroelectric facilities. A multi-objective optimization strategy was inspected by [23] to investigate the coordinated scheduling of the integrated EV systems and wind generation units, which aimed at improving the wind power adsorption and energy conservancy of the thermal units. A risk-averse optimal scheduling framework is investigated in [24] for smart parking lots in electricity market trading considering electricity price fluctuations. In [25], a hybrid stochastic-robust scheduling is studied for the interaction of smart parking lots with competitive electricity markets in a distributed framework. In this research, the ADMM algorithm is used to achieve the overall equilibrium point. Study [26] has designed a fuzzy logic controller for coordination of EVs in EDNs, which leads to the minimization of operating costs, flattening of the voltage profile and reduction of emissions. A hybrid stochastic-robust model is investigated in [27] for the optimal day ahead scheduling of plug-in electric vehicles connected to the EDN in the presence of RESs.

Although studies [28–30] have not included EVs in their framework, they have made notable contributions in bi-level optimization concerning power system studies. Particularly, [28] investigated a risk-averse and risk-seeker price-maker optimization framework for Disco to engage in WEM The alternating direction method of multipliers (ADMM) was deployed by [29] to solve the bi-level optimization problem for price-maker microgrids that participate in LEM. In particular, the study deployed robust optimization (RO) to deal with uncertain data. Furthermore, a novel Dantzig–Wolfe decomposition technique was introduced by [30] to solve the optimal price-maker scheduling of multiple microgrids in WEM, while the study integrated an RO-SP method to deal with uncertain data. A bi-level optimization approach is discussed in [31] for strategic participation of Disco in day-ahead and real-time wholesale market.

A hybrid Stackelberg–Nash mechanism is presented in [32] for decentralized trading of smart homes with Disco. In this study, ADMM algorithm is used to achieve the equilibrium of energy exchanged between players. In [33], a bi-level optimization approach based on risk management is proposed for the strategic participation of the Disco in the day-ahead WEM. In this study, the Disco and the WEM are modelled at the upper and lower levels of the problem, respectively. A bi-level approach based on game theory is investigated in [34] for trading between microgrids and electrical distribution network (EDN). In this study, the SP method is used to model the uncertain behaviour of uncertainty parameters. A bi-level optimization framework is proposed in [35] for decentralized trading of smart parking lots, LEM and multiple microgrids. In this study, the DRO method has been used to model the uncertain behaviour of RESs. In [36], a hybrid stochastic-robust scheduling is proposed for the participation of EV aggregators in the WEM as a strategic player. In this study, EV aggregators and WEM are modelled at the upper and lower levels of the problem, respectively. A hybrid stochastic-robust framework is presented in [37] to investigate the effects of smart charging in an active EDN. In [38], a convex optimization framework is proposed to investigate the impact of smart charging and uncontrolled charging in multi-energy EDN considering flexible energy sources. In this study, the hybrid stochastic-robust method is used to model the uncertain behaviour of the uncertainty parameters.

1.3. Contribution

Table 1 gives a comprehensive taxonomic evaluation on the main characteristics of the current literature and this study. Aside from the timely contributions of all the aforementioned studies, the following under-researched aspects stand out:

a The studies [16,17,19–21,23–26,29,32,34,35,37,38] have adopted a price-taker market participation strategy approach. However, a higher level of profit can be obtained if a price-maker market model was adopted to give offers/bids and be an active part of the market.

b In bi-level studies [18,20,21,26,28,35,37–39], the participation strategies in LEM is studied, while publications [28,31], and [33] have studied the scheduling strategies of Disco in WEM as a price-maker. Nevertheless, the price-maker framework has not been addressed for both LEM and WEM simultaneously, which requires a tri-level optimization method.

c The SP method has been deployed by [20,31,33], while studies [28,29] proposed RO models to deal with uncertain parameters of real-world conditions. Although [25,27,30,36–38] have used a hybrid RO-SP strategy to deal with some uncertainties, this novel method has not been applied for handling uncertain nature of EVs and SDG production intermittency. Furthermore, EVs' uncertainty is neglected in [16,17,19,21,23,26,32].

d The power system models have a great significance as they consider the system's constraints, such as voltage, current and congestion. However, the studies [16,17], and [23] lack the power system models.

To address these existing gaps in the literature, this study puts forward a novel tri-level optimization framework for IEVSDGs to take part in LEM and WEM. The IEVSDGs form the first level of the problem and they consist of smart urban EV parking lots that are integrated with SDGs. The IEVSDGs' operator at the ADS level receives the distribution of the uncertain data, e.g., solar power production, arrival/departure time and daily travelled miles of EVs. Subsequently, the EVs are clustered into fleets (EVF) according to their empirical probability distribution functions via the k-means clustering method. At this stage, the IEVSDGs operator schedules the charge/discharge patterns of the EVFs as well as the solar energy dispatch and strategically submits the offers/bids in the LEM, which is modelled by IEEE 69-bus ADS. At the second level, the Disco operator self-schedules and clears LEM to minimize the operational costs, which is the reason why IEVSDGs' behaviour is considered as strategic since it includes the possible response of the market to the submitted energy offer/bid. However, to procure part of its energy, the Disco also partakes in WEM, which is modelled by IEEE 24-bus transmission network (TN). When the Disco submits its offers/bids in WEM (the third level of the problem), the WEM operator clears the market and announces the MCP of WEM.

In summation, the behaviour of the Disco in WEM is also strategic and the proposed problem has double layers of strategic behaviour since the IEVSDGs is a strategic price-maker in LEM, while the LEM operator (that is Disco) is also a strategic price-maker in WEM. In other words, the Disco is an intermediary link that connects IEVSDGs to WEM. To solve this three-level optimization problem this study combines ADMM and KKT conditions, which to the best of authors' knowledge, have not been studied in previous publications. Additionally, this work deploys a hybrid RO-SP approach to deal with uncertain data to benefit the advantages of the both methods. For instance, the RO provides more reasonable results with erratic parameters, such as solar production, while the parameters that have certain probability distribution functions, i.e., EVFs behavioural patterns, are better handled with SP. Overall, the original contributions of this study can be listed as follows:

i A novel tri-level optimization framework is proposed for IEVSDGs to take part in LEM as a strategic price-maker, while considering that Disco is also and strategic price-maker in WEM.
ii The study combines KKT and ADMM methods to solve the tri-level optimization problem.
iii An effective hybrid RO-SP method is deployed to deal with uncertainties that are derived from EVFs' behavioural patterns and SDG production.

2. Problem description

In the proposed model, the IEVSDG is the first-level optimization problem. The IEVSDGs' operator is obliged to coordinate EVFs and SDGs intending to minimize their collective operational costs. The uncertain data set corresponding to EVFs' arrival/departure times, and travelled distance before reaching the smart parking lot, are modelled based on scenario-based stochastic programming (SP), while the solar energy is a rather erratic parameter, which is therefore defined by RO models to handle its uncertain nature. More information on this hybrid RO-SP method is included in [40]. At first stage, the IEVSDG submits the offers/bids in LEM, which is operated by the Disco and forms the second level problem. Then the Disco operator is an intermediary retailer between the IEVSDG and WEM. Accordingly, the Disco operator submits its offers/bids in WEM, which is designated as the third level problem, whose objective is achieving the highest possible public satisfaction. In other words, the proposed model provides the best LEM participation strategy for IEVSDG considering that its operator (Disco) is also trying to achieve the best market strategy at WEM, and WEM has the goal of maximizing social satisfaction. The general structure of the tri-level problem, interactions of different operators and system components are depicted by Fig. 1.

3. Formulation & algorithm

3.1. Integrated electric vehicle fleets and solar distributed generations (first level)

In this study, the EVs are clustered into fleets (EVF) via the k-means clustering method as it is presented in [41], and they are assumed to be in idle mode from the arrival to the parking lot to their departure time. The vehicles' arrival/departure and daily travelled miles are uncertainties that follow certain distributions, and are handled by finite scenarios for each EVF in the SP approach. The IEVSDG forms the first level of the problem, and it consists of smart EV parking lots and SDGs. The SP objective of the IEVSDG operator can be observed in Eq. (1), which contains the cost of taking part in LEM, the EVFs' battery degradation and operational costs of SDGs. After forming this SP problem, the RO is adopted to deal with SDG production uncertainties, which is described in Appendix D. The state of charge (SOC) of each fleet at their arrival time to the parking lot and other periods is defined by Eqs. (2)–(3), respectively. The first term in Eq. (3) illustrates the initial value of SOC when EVFs arrive as a function of their daily travelled miles and minimum allowed SOC. The bound of the SOC at departure (when vehicle leaves the lot) is enforced by Eq. (4), which ensures that EVFs have required amount of charge at the departure time. The min/max restrictions for SOC and charge/discharge power are declared by Eqs. (5)–(6), respectively. The binary constraint Eq. (7) prevents the actions of simultaneous charge/discharge. Moreover, the cycle depth, the cycle depth degradation cost function, and marginal degradation are established in Eqs. (8)–(10). The overall battery degradation in each time step is derived from Eq. (11) [42], which is a nonlinear equation, and its linearization is elaborated in Appendix C. Further details on the battery degradation cost function are included [43]. Eqs. (12)–(16) illustrate the robust solar power model, Eventually, the exported/imported electrical energy from LEM is established through Eq. (17).

$$OF_1 = min \sum_{s} \pi_s \sum_{t} \sum_{v,i\in A_i^v} \begin{pmatrix} \left(p^{+}_{v,s,t} - p^{-}_{v,s,t} - p^{pv}_{v,s,t}\right) \lambda^{LEM*}_{t,i} \\ +dg^{Lin}_{v,s,t} + c^{pv}_{v} p^{pv}_{v,s,t} \end{pmatrix} \tag{1}$$

$$SOC_{v,s,t} = SOC_{v,s,t-1} + \left(\eta_v . p^{+}_{v,s,t}/EB_v\right) - \left(p^{-}_{v,s,t}/EB_v . \eta_v\right) \forall v, s, t \neq TA_{s,v} \tag{2}$$

$$SOC_{v,s,t} = \max\left(\underline{SOC_v}, 1 - (DT_{v,s} \times EM_v/EB_v)\right) + \left(\eta_v . p^{+}_{v,s,t}/EB_v\right) - \left(p^{-}_{v,s,t}/EB_v . \eta_v\right) \quad \forall v,s,t = TA_{s,v} \tag{3}$$

$$SOC_{v,s,t} = \min\left(SOC^{end}_{v,s}, SOC^{des}_{v}\right), \forall v, s, t = TD_{v,s} \tag{4}$$

$$\underline{SOC_v} \leq SOC_{v,s,t} \leq \overline{SOC_v} \forall v, s, t \tag{5}$$

$$p^{+}_{v,s,t} \leq Cr_v . uc_{v,s,t}, p^{-}_{v,s,t} \leq Cr_v . ud_{v,s,t} \forall v, s, t \tag{6}$$

$$uc_{v,s,t} + ud_{v,s,t} \leq 1 \forall v, s, t \tag{7}$$

$$\sigma_{v,s,t} = \sigma_{v,s,t-1} - (p^{-}_{v,s,t}/EB_v . \eta_v) \forall v, s, t \tag{8}$$

$$\psi_{v,s,t}\left(\sigma_{v,s,t}\right) = a_0 . \left(\sigma_{v,s,t}\right)^{2.03} \forall v, s, t \tag{9}$$

$$MD_{v,s,t} = 2.03 a_0 (BC_v/EB_v . \eta_v) {\sigma_{v,s,t}}^{1.03} \forall v, s, t \tag{10}$$

$$dg^{Nl}_{v,s,t} = p^{-}_{v,s,t} . MD_{v,s,t} \forall v, s, t \tag{11}$$

$$0 \leq p^{pv}_{v,s,t} \leq \overline{p^{pv}_{v,t}} \forall v, s, t \tag{12}$$

Table 1
Comparative evaluations between this study and previous works.

Ref	IEVSDG	LEM	WEM	Smart charge	Strategic behaviour	Model	Algorithm	Uncertainty
[16]	✓	×	×	✓	Price taker	Single level	×	×
[17]	✓	×	×	✓	Price taker	Single level	×	×
[18]	✓	✓	×	×	Price maker	Bi-level	KKT	×
[19]	✓	✓	×	✓	Price taker	Single level	PSO	×
[20]	✓	✓	×	×	Price taker	Bi-level	Two stage	SP
[21]	✓	✓	×	×	Price taker	Bi-level	Two stage	×
[22]	✓	×	✓	×	Price maker	Bi-level	KKT	DRO
[23]	✓	×	×	×	Price taker	Single level	×	×
[24]	✓	✓	×	✓	Price taker	Single level	×	CVaR
[25]	✓	×	✓	×	Price taker	Bi-level	ADMM	SP-RO
[26]	✓	✓	×	✓	Price taker	Single level	×	×
[27]	✓	✓	×	×	Price taker	Single level	×	SP-RO
[28]	×	✓	✓	×	Price maker	Bi-level	KKT	IGDT
[29]	×	✓	×	×	Price taker	Bi-level	ADMM	RO
[30]	×	×	✓	×	Price maker	Bi-level	Dantzig–Wolfe	SP-RO
[31]	×	✓	✓	×	Price maker	Bi-level	KKT	SP
[32]	×	✓	×	×	Price taker	Bi-level	ADMM+ benders	×
[33]	×	✓	✓	×	Price maker	Bi-level	KKT	CVaR
[34]	×	✓	×	×	Price taker	Bi-level	Game theory	SP
[35]	✓	✓	×	✓	Price taker	Bi-level	ADMM	DRO
[36]	✓	×	✓	✓	Price maker	Bi-level	KKT	SP-RO
[37]	✓	✓	×	✓	Price taker	Single level	×	SP-RO
[38]	✓	✓	×	✓	Price taker	Single level	×	SP-RO
This paper	✓	✓	✓	✓	Price maker	Tri-level	KKT+ADMM	SP-RO

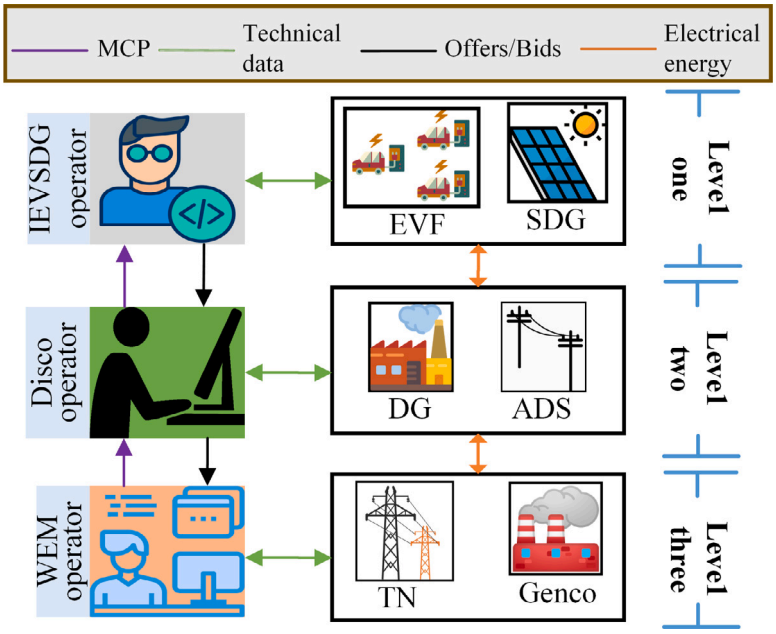

Fig. 1. Overall structure of the tri-level problem.

$$p^{pv}_{v,s,t} - x^{RO}_{v,s,t}\overline{p^{pv}_{v,t}} + z^{RO}_{v,s,t} I^{RO} + p^{RO}_{v,s,t} \le 0 \forall v, s, t \quad (13)$$

$$z^{RO}_{v,s,t} + p^{RO}_{v,s,t} \ge \hat{p}^{pv}_{v,s,t} y^{RO}_{v,s,t} \forall v, s, t \quad (14)$$

$$-y^{RO}_{v,s,t} \le x^{RO}_{v,s,t} \le y^{RO}_{v,s,t} \forall v, s, t \quad (15)$$

$$y^{RO}_{v,s,t}, p^{RO}_{v,s,t}, z^{RO}_{v,s,t} > 0, x^{RO}_{v,s,t} = 1 \forall v, s, t \quad (16)$$

$$\vec{P}^{ES}_{t,v} - \overleftarrow{P}^{ES}_{t,v} = \sum_{s} \pi_s . (p^{pv}_{v,s,t} - p^{+}_{v,s,t} + p^{-}_{v,s,t}) \forall t, v \quad (17)$$

3.2. Distribution company (second level)

3.2.1. DG's commitment

The Disco is an intermediary body that facilitates the energy transactions between the IEVSDG and WEM. The Disco's objective is established in Eq. (18), which contains the cost of the energy purchased/sold in WEM, the IL cost and DG-related costs, such as their operation cost and start-up/shutdown costs. The multiplication nonlinearities in Eq. (18) are dealt with via the theory of strong duality according to [44]. Eventually, the last expression in the objective function represents the cost/benefit of transacting energy with IEVSDG (first level). The commitment schedule of the DGs (adopted from [45]) is clarified through Eq. (19), while Eq. (20) expresses the fuel cost associated with starting the DGs up or shutting them down. The ramp up/down rate restrictions are constrained via Eqs. (21)–(22). The start-up/shutdown

time requirements at the initial and final time steps of the scheduling period are established in Eqs. (23)–(24), while they are enforced by Eqs. (24)–(28) for various scheduling horizons, e.g., beginning, middle and final time intervals. Moreover, the on/off modes of DGs are determined through binary equality in Eq. (29).

$$OF_2 = min \sum_{t} \left\{ \begin{array}{l} \sum\limits_{b \in A_b^{Ds}} \lambda_{b,t}^{WEM} p_t^{Dsc} + \sum\limits_{l} C_l^{IL} p_{l,t}^{IL} \\ + \sum\limits_{k} \left(C_k^{DG} P_{k,t}^{DG} + \widehat{S}_{k,t} + \breve{S}_{k,t} \right) \\ + \sum\limits_{v,i \in A_i^v} \overleftrightarrow{P}_{v,t}^{ES} \lambda_{t,i}^{LEM*} \end{array} \right\} \quad (18)$$

$$\underline{p_k^{DG}} I_{k,t} \le p_{k,t}^{DG} \le \overline{p_k^{DG}} I_{k,t} \forall t, k \quad (19)$$

$$\widehat{S}_{k,t} \ge C_k^{\widehat{S}} y_{k,t}, \breve{S}_{k,t} \ge C_k^{\breve{S}} z_{k,t} \forall t, k \quad (20)$$

$$p_{k,t}^{DG} - p_{k,t-1}^{DG} \le (1 - y_{k,t}) \widehat{R}_k + y_{i,t} \underline{p_k^{DG}} \forall t, k \quad (21)$$

$$p_{k,t-1}^{DG} - p_{k,t}^{DG} \le (1 - z_{k,t}) \breve{R}_k + z_{i,t} \underline{p_k^{DG}} \forall t, k \quad (22)$$

$$T_k^{Ue} = \min \left\{ T, T_k^{U0} \right\}, T_k^{De} = \min \left\{ T, T_k^{D0} \right\} \forall k \quad (23)$$

$$\sum_{t=1}^{T_k^{Ue}} I_{k,t} = T_k^{Ue}, \sum_{t=1}^{T_k^{De}} I_{k,t} = 0 \forall k \quad (24)$$

$$\sum_{t=r}^{t+T_k^{Ue}-1} I_{k,r} \ge T_k^U y_{k,t} \forall k, \forall t = \left[T_k^{Ue} + 1, \ldots, T - T_k^U + 1 \right] \quad (25)$$

$$\sum_{t=r}^{T} (I_{k,r} - y_{k,t}) \ge 0 \forall k, \forall t = \left[T - T_k^U + 2, \ldots .., T \right] \quad (26)$$

$$\sum_{t=r}^{t+T_k^D-1} (1 - I_{k,r}) \ge T_k^D z_{k,t} \forall k, \forall t = \left[\begin{array}{l} T_k^{De} + 1, \ldots ., \\ T - T_k^D + 1 \end{array} \right] \quad (27)$$

$$\sum_{t=r}^{T} (1 - I_{k,r} - z_{k,t}) \ge 0 \forall k, \forall t = \left[\begin{array}{l} T - T_k^D \\ +2, \ldots ., T \end{array} \right] \quad (28)$$

$$\begin{array}{l} y_{k,t} - z_{k,t} = I_{k,t\,-\,1} - I_{k,t} \\ y_{k,t} + z_{k,t} \leqslant 1 \ \forall t,k \end{array} \quad (29)$$

3.2.2. Active distribution system

This study has adopted the ADS model from [44]. The feeders' power flow is calculated by Eq. (30), while Eqs. (31)–(32) define their corresponding power loss and current flow. The bounds of voltage/current values are circumscribed by Eq. (33). The Eq. (34) models the active power limit that can be transmitted from the feeders. Eventually, the power equilibrium in slack node and other nodes is introduced by Eqs. (35)–(36) [46]. It is noteworthy that the dual variable associated with Eq. (36) defines the local market price ($\lambda_{t,i}^{LEM}$). Eventually, Eq. (37) expresses the constraint that connects the first level variables to the second level variables.

$$P_{ij,t}^{flow} = \left(R_{ij}^{DS} / (Z_{ij}^{DS})^2 \right) . (\widehat{V}_{i,t}^{DS} - \widehat{V}_{j,t}^{DS}) \forall ij, \forall t \quad (30)$$

$$P_{ij,t}^{Loss} = R_{ij}^{DS} \widehat{I}_{ij}^{DS} \forall ij, \forall t \quad (31)$$

$$I_{ij,t}^{DS} = (V_{i,t}^{DS} - V_{j,t}^{DS}) / Z_{ij}^{DS} \forall ij, \forall t \quad (32)$$

$$-\overline{I_{ij}^{DS}} \le I_{ij,t}^{DS} \le \overline{I_{ij}^{DS}}, \underline{V_i^{DS}} \le V_{i,t}^{DS} \le \overline{V_i^{DS}} \forall ij, \forall t \quad (33)$$

$$-\overline{P_{ij,t}^{flow}} \leqslant P_{ij,t}^{flow} \leqslant \overline{P_{ij}^{flow}} \forall ij, \forall t \quad (34)$$

$$\begin{array}{l} p_t^{Dsc} + \sum\limits_{k \in A_i^k} P_{k,t}^{DG} + \sum\limits_{l \in A_i^l} P_{l,t}^{IL} + \sum\limits_{v \in A_i^v} \overleftrightarrow{P}_{v,t}^{ES} = \sum\limits_{d \in A_i^d} P_{d,t}^{DSL} \\ +0.5(\sum\limits_{j \in DS} P_{ij,t}^{Loss} + \sum\limits_{j \in DS} P_{ij,t}^{flow}) \forall i = 1, \forall t \end{array} \quad (35)$$

$$\begin{array}{l} \sum\limits_{k \in A_i^k} P_{k,t}^{DG} + \sum\limits_{l \in A_i^l} P_{l,t}^{IL} + \sum\limits_{v \in A_i^v} \overleftrightarrow{P}_{v,t}^{ES} = \sum\limits_{d \in A_i^d} P_{d,t}^{DSL} \\ +0.5(\sum\limits_{j \in DS} P_{ij,t}^{Loss} + \sum\limits_{j \in DS} P_{ij,t}^{flow}) : \lambda_{t,i}^{LEM}, \forall i \ne 1, \forall t \end{array} \quad (36)$$

$$\overleftrightarrow{P}_{v,t}^{ES} = \vec{P}_{t,v}^{ES} - \overleftarrow{P}_{t,v}^{ES}, \forall t, \forall v \quad (37)$$

3.3. Wholesale electricity market (third level)

The WEMO's objective is expressed by Eq. (38), where the first term corresponds to the Genco operation cost, while the second term is the cost/benefit of transacting with Disco. Furthermore, the nodal energy equilibrium is satisfied by Eqs. (39)–(40). Moreover, the dual variables of these equality constraints ($\lambda_{b,t}^{WEM}$) represent the MCP in WEM. The capacity limits of the Gencos is imposed by Eq. (41). In this study, the block offering model is adopted for Gencos from [47], and Eq. (42) characterizes the bounds of each production block. The ramp rate restrictions of the Gencos are established by Eqs. (43)–(46). Eq. (47) restricts the transaction limits between Disco and WEM, and the wind farm limit are defined by Eq. (48). The limitation of transmission lines is also modelled by Eq. (49). The voltage angle of the nodes are limited within the nominal bounds through Eq. (50). The overall generation of the Gencos is equal to the summation of all their piece-wise segments, which is defined via Eq. (51). Ultimately, the voltage angle of the slack node is fixed as the reference node in Eq. (52).

$$OF_3 = \min \sum_{t} \left\{ \sum_{g} \sum_{m} C_{g,m}^{G} \rho_{g,m,t}^{G} - C_t^{Dsc} p_t^{Dsc} \right\} \quad (38)$$

$$\begin{array}{l} \sum\limits_{g \in A_b^g} P_{g,t}^{G} + \sum\limits_{w \in A_b^w} P_{w,t}^{WT} - P_t^{Dsc} = \sum\limits_{b' \in Tr} B_{b,b'} (\delta_{b,t} - \delta_{b',t}) : \lambda_{b,t}^{WEM} \\ \forall b \in A_b^{Ds}, \forall t \end{array} \quad (39)$$

$$\begin{array}{l} \sum\limits_{g \in A_b^g} P_{g,t}^{G} + \sum\limits_{w \in A_b^w} P_{w,t}^{WT} - \sum\limits_{d \in A_b^d} P_{d,t} = \sum\limits_{b' \in Tr} B_{b,b'} (\delta_{b,t} - \delta_{b',t}) : \lambda_{b,t}^{WEM} \\ \forall b \notin A_b^{Ds}, \forall t \end{array} \quad (40)$$

$$0 \le P_{g,t}^{G} \le \bar{P}_{g,t} : \overline{\mu_{g,t}^1}, \underline{\mu_{g,t}^1} \forall g, \forall t \quad (41)$$

$$0 \le \rho_{g,m,t}^{G} \le \bar{\rho}_{g,m} : \overline{\mu_{g,m,t}^2}, \underline{\mu_{g,m,t}^2} \forall g, \forall m, \forall t \quad (42)$$

$$P_{g,t}^{G} - P_{g,t-1}^{G} \le RU_g : \mu_{g,t}^3 \forall g, \forall t > 1 \quad (43)$$

$$P_{g,t}^{G} - P_{g,ini}^{G} \le RU_g : \mu_{g,t}^4 \forall g, \forall t = 1 \quad (44)$$

$$P_{g,t-1}^{G} - P_{g,t}^{G} \le RD_g : \mu_{g,t}^5 \forall g, \forall t > 1 \quad (45)$$

$$P_{g,ini}^{G} - P_{g,t}^{G} \le RD_g : \mu_{g,t}^6 \forall g, \forall t = 1 \quad (46)$$

$$\underline{p_t^{Dsc}} \le p_t^{Dsc} \le \overline{p_t^{Dsc}} : \overline{\mu_t^7}, \underline{\mu_t^7}, \forall t \quad (47)$$

$$0 \leqslant P^{\mathrm{WT}}_{\mathrm{w,t}} \leqslant \overline{P^{\mathrm{WT}}_{\mathrm{w,t}}} : \overline{\mu^{8}_{\mathrm{w,t}}}, \underline{\mu^{8}_{\mathrm{w,t}}} \forall \mathrm{w}, \forall \mathrm{t} \tag{48}$$

$$-C^{\mathrm{Max}}_{\mathrm{b,b'}} \leq B_{\mathrm{b,b'}}(\delta_{\mathrm{b,t}} - \delta_{\mathrm{b',t}}) \leq C^{\mathrm{Max}}_{\mathrm{b,b'}} : \underline{\upsilon_{\mathrm{b,b',t}}}, \overline{\upsilon_{\mathrm{b,b',t}}} \quad \forall \mathrm{b}, \forall \mathrm{b'}, \forall \mathrm{t} \tag{49}$$

$$-\pi \leq \delta_{\mathrm{b,t}} \leq \pi : \underline{\xi_{\mathrm{b,t}}}, \overline{\xi_{\mathrm{b,t}}} \forall \mathrm{b}, \forall \mathrm{t} \tag{50}$$

$$\sum_{\mathrm{m}} \rho^{\mathrm{G}}_{\mathrm{g,m,t}} = P^{\mathrm{G}}_{\mathrm{g,t}} : \lambda^{1}_{\mathrm{g,t}} \forall \mathrm{g}, \forall \mathrm{t} \tag{51}$$

$$\delta_{\mathrm{b=ref,t}} = 0 : \xi^{l}_{\mathrm{b=ref,t}} \forall \mathrm{b}, \forall \mathrm{t} \tag{52}$$

3.4. Algorithm

In the proposed model, the Disco is an intermediary entity between the IEVSDGs and WEM and its' sole duty is to procure energy for the customers. In this respect, it endeavours to self-schedule the local DGs and submit the most suitable offer/bid in WEM and provide the best price to IEVSDGs. The WEM operator receives all the offers/bids and independently clears the market to maximize community wealth. Accordingly, the Disco scheduling must be of a tactical (strategic) nature, as it must anticipate its possible impact on the market as a price-maker, which makes the second and third-level problems a bi-level model. On the other hand, the IEVSDG operator has a similar kind of transactional relationship with Disco at the local market level. That is to say the IEVSDG operator self-schedules and submits offers/bids at the LEM level as a tactical price-maker since it takes the possible response of the market into consideration. In summation, the IEVSDG is a tactical price-maker at local level, which considers that Disco is also a tactical player at the WEM level. In Fig. 2, the overall schematic of the proposed tri-level optimization problem is illustrated. The participation of the Disco in WEM forms the second and third level problems, which is a bi-level problem. Since this problem has a convex lower-level, the KKT conditions are adopted in this study (see [48]) to achieve the best equilibrium point, which converts the second (Disco) and third level (WEM) problems into a single-objective optimization model. The KKT conditions of this study are included in Appendices A and B elaborates on the theory of strong duality. After merging the second and third levels in single-level problem, the first-level and this merged problem create another two-level optimization problem as it is illustrated in Fig. 1. Since this problem is a complicated non-convex MILP, we could not use the KKT conditions again to solve this problem. In this regard this problem was solved by ADMM, which is a powerful new iterative algorithm with fast convergence. The details of achieving the overall equilibrium point through the hybrid ADMM algorithm and KKT condition are as follows.

In general, an optimization problem can be solved by ADMM in following decomposable format:

$$\min_{x\in X, z\in Z} f(x) + g(z) \tag{53}$$

s.t

$$Ax + Bz = c \tag{54}$$

The augmented lagrangian function of the Eqs. (53), and Eq. (54) is defined by Eq. (55), where λ is known as the lagrangian multiplier (which is the local electricity market price in our problem), while $\|.\|$ denotes the penalty term in the form second order norm vector. The ADMM is comprised of repeating Eqs. (53)–(58), where k represents the index of iterations (or repetitions in a loop). As a result, Eq. (56) and (57) are solved separately, which makes the ADMM a powerful decentralized solving method.

$$L(x, z, \lambda) = f(x) + g(z) + \lambda^{T}(Ax + Bz - c) + (\rho/2)\|Ax + Bz - c\|_2^2 \tag{55}$$

$$x(k+1) = \arg\min_{x\in X} L(x, z(k), \lambda(k)) \tag{56}$$

$$z(k+1) = \arg\min_{z\in Z} L(x(k+1), z, \lambda(k)) \tag{57}$$

$$\lambda(k+1) = \lambda(k) + \rho(Ax(k+1) + Bz(k+1) - c) \tag{58}$$

The convergence of the ADMM is defined based on the primal residuals, which is defined as follows:

$$\|\lambda(k+1) - \lambda(k)\| \leq \varepsilon \tag{59}$$

According to Eq. (53), we assume that $f(x)$ expresses the objective function of IEVSDGs and x is also the decision variables related to IEVSDGs. On the other hand, it is assumed that $g(z)$ expresses the objective function of LEM and z shows the decision variable of LEM. Now, according to the explanations given, Eq. (53) can be reformulated by the integrated approach Eq. (60):

$$\min \sum_{s} \pi_{\mathrm{s}} \sum_{t} \left(\begin{array}{l} \sum_{v} CEV_{v,t} + \sum_{\mathrm{b}\in \mathrm{A}^{\mathrm{Ds}}_{\mathrm{b}}} \lambda^{\mathrm{WEM}}_{\mathrm{b,t}} p^{\mathrm{Dsc}}_{\mathrm{t}} + \sum_{\mathrm{l}} C^{\mathrm{IL}}_{\mathrm{l}} p^{\mathrm{IL}}_{\mathrm{l,t}} \\ + \sum_{\mathrm{k}} \left(C^{\mathrm{DG}}_{\mathrm{k}} P^{\mathrm{DG}}_{\mathrm{k,t}} + \widehat{S}_{\mathrm{k,t}} + \breve{S}_{\mathrm{k,t}} \right) \end{array} \right) \tag{60}$$

Where $CEV_{v,t} = dg^{\mathrm{Lin}}_{\mathrm{v,s,t}} + c^{\mathrm{pv}}_{\mathrm{v}} p^{\mathrm{pv}}_{\mathrm{v,s,t}}$ represents the operating cost of IEVSDGs in integrated mode with the Disco. In other words, in Eq. (60), the owner of IEVSDGs is the Disco, and the privacy of IEVSDGs is not respected in trading with Disco.

In the proposed approach, Eq. (54) can also be reformulated by Eq. (61).

$$\overleftrightarrow{P}^{\mathrm{ES}}_{\mathrm{v,t}} = \vec{P}^{\mathrm{ES}}_{\mathrm{t,v}} - \overleftarrow{P}^{\mathrm{ES}}_{\mathrm{t,v}} \qquad \forall v, \forall t \tag{61}$$

Now, according to Eq. (60), Eq. (55) and (61), the augmented Lagrangian function of the proposed approach can be obtained by equation Eq. (62):

$$\begin{aligned} &L(x, z, \lambda) = \\ &\min \sum_{s} \pi_{\mathrm{s}} \sum_{t} \\ &\left(\underbrace{\sum_{v} CEV_{v,t}}_{f(x)} + \underbrace{\sum_{\mathrm{b}\in \mathrm{A}^{\mathrm{Ds}}_{\mathrm{b}}} \lambda^{\mathrm{WEM}}_{\mathrm{b,t}} p^{\mathrm{Dsc}}_{\mathrm{t}} + \sum_{\mathrm{l}} C^{\mathrm{IL}}_{\mathrm{l}} p^{\mathrm{IL}}_{\mathrm{l,t}} + \sum_{\mathrm{k}} \left(C^{\mathrm{DG}}_{\mathrm{k}} P^{\mathrm{DG}}_{\mathrm{k,t}} + \widehat{S}_{\mathrm{k,t}} + \breve{S}_{\mathrm{k,t}} \right)}_{g(z)} \right. \\ &\left. + \underbrace{\lambda^{\mathrm{LEM}}_{\mathrm{t,i}} \left(\overleftrightarrow{P}^{\mathrm{ES}}_{\mathrm{v,t}} - \left(\vec{P}^{\mathrm{ES}}_{\mathrm{t,v}} - \overleftarrow{P}^{\mathrm{ES}}_{\mathrm{t,v}} \right) \right)}_{\lambda^{T}(Ax+Bz-c)} + \underbrace{(\rho/2) \cdot \left\| \overleftrightarrow{P}^{\mathrm{ES}}_{\mathrm{v,t}} - \left(\vec{P}^{\mathrm{ES}}_{\mathrm{t,v}} - \overleftarrow{P}^{\mathrm{ES}}_{\mathrm{t,v}} \right) \right\|_2^2}_{(\rho/2)\|Ax+Bz-c\|_2^2} \right) \end{aligned} \tag{62}$$

As it was mentioned, equation Eq. (62) can be decomposed to solve IEVSDG and LEMP problems in a decentralized form (two separate problems). The iterative ADMM algorithm is illustrated in Fig. 2, as it is implemented in following steps:

Algorithm: Tri-level equilibrium

Initialization: Receive the input parameters for first, second and third level problems.

1. Choose a penalty rate (ρ) and a convergence threshold (ε). Provide a random value for energy bidding ($\lambda^{\mathrm{LEM}*}_{\mathrm{t,i}}$) and energy trade between IEVSDG and LEM (which is $\overleftrightarrow{P}^{\mathrm{ES}}_{\mathrm{v,t}}$).

2. Solve the optimization problem of the IEVSDG based on the value of ($\lambda^{\mathrm{LEM}*}_{\mathrm{t,i}}$) and ($\overleftrightarrow{P}^{\mathrm{ES}}_{\mathrm{v,t}}$) as follows:

$$x(k+1) = \arg\min_{x\in X} \sum_{\mathrm{s}} \pi_{\mathrm{s}} \sum_{\mathrm{t}} \sum_{v,i\in \mathrm{A}^{\mathrm{v}}_{\mathrm{i}}}$$

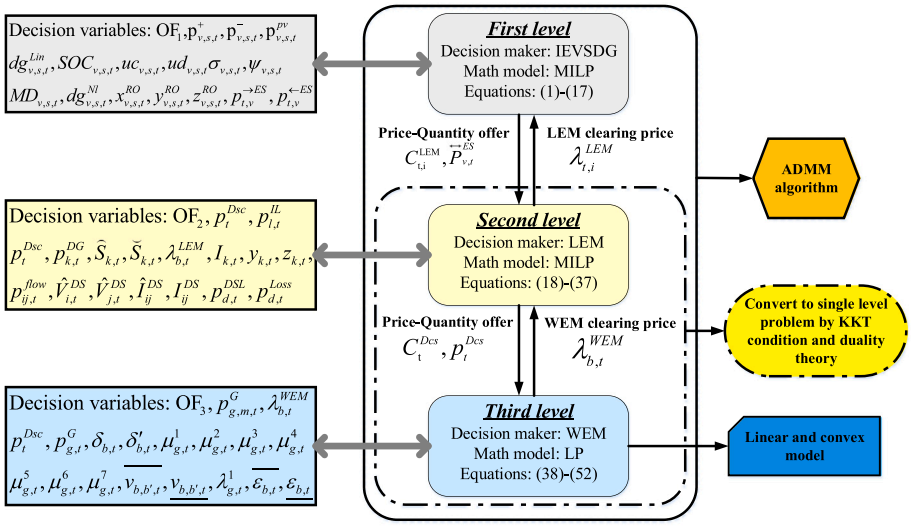

Fig. 2. The general structure of the proposed algorithm from the concept and mathematics point of view.

$$\times\left\{\begin{array}{l} dg^{\mathrm{Lin}}_{\mathrm{v,s,t}}+c^{\mathrm{pv}}_{\mathrm{v}}p^{\mathrm{pv}}_{\mathrm{v,s,t}}-\left(\vec{P}^{\mathrm{ES}}_{\mathrm{t,v}}-\overleftarrow{P}^{\mathrm{ES}}_{\mathrm{t,v}}\right)\lambda^{\mathrm{LEM}*}_{\mathrm{t,i}}(k) \\ +\rho.\left\|\overleftrightarrow{P}^{\mathrm{ES}*}_{\mathrm{v,t}}(k)-\left(\vec{P}^{\mathrm{ES}}_{\mathrm{t,v}}-\overleftarrow{P}^{\mathrm{ES}}_{\mathrm{t,v}}\right)\right\|^{2}_{2} \end{array}\right. \tag{63}$$

Subject to: Eqs. (2)–(17)

3. Update $\vec{P}^{\mathrm{ES}*}_{\mathrm{t,v}}(\mathrm{k})$ and $\overleftarrow{P}^{\mathrm{ES}*}_{\mathrm{t,v}}(\mathrm{k})$ from the solution.

4. Merge the second and third level problems in single problem using the conditions of KKT. Please refer to Appendices A and B for the details of this step.

5. Solve the LEM problem using the obtained fixed inputs $\vec{P}^{\mathrm{ES}*}_{\mathrm{t,v}}(\mathrm{k})$ and $\overleftarrow{P}^{\mathrm{ES}*}_{\mathrm{t,v}}(\mathrm{k})$ as follows:

$$z(k+1)=\arg\min_{z\in Z}\sum_{\mathrm{t}}$$
$$\times\left\{\begin{array}{l} \sum\limits_{\mathrm{b}\in\mathrm{A}^{\mathrm{Ds}}_{\mathrm{b}}}\lambda^{\mathrm{WEM}}_{\mathrm{b,t}}p^{\mathrm{Dsc}}_{\mathrm{t}}+\sum\limits_{\mathrm{l}}C^{\mathrm{IL}}_{\mathrm{l}}p^{\mathrm{IL}}_{\mathrm{l,t}}+\sum\limits_{\mathrm{k}}\left(C^{\mathrm{DG}}_{\mathrm{k}}P^{\mathrm{DG}}_{\mathrm{k,t}}+\widehat{S}_{\mathrm{k,t}}+\breve{S}_{\mathrm{k,t}}\right) \\ +\sum\limits_{v,i\in\mathrm{A}^{\mathrm{v}}_{\mathrm{i}}}\overleftrightarrow{P}^{\mathrm{ES}}_{\mathrm{v,t}}\lambda^{\mathrm{LEM}*}_{\mathrm{t,i}}(k)-\rho.\left\|\overleftrightarrow{P}^{\mathrm{ES}*}_{\mathrm{v,t}}-\left(\vec{P}^{\mathrm{ES}}_{\mathrm{t,v}}(k+1)-\overleftarrow{P}^{\mathrm{ES}}_{\mathrm{t,v}}(k+1)\right)\right\|^{2}_{2} \end{array}\right\} \tag{64}$$

Subject to: Eqs. (19)–(52) and Eqs.(a.1)-(a.21)

6. Update $\overleftrightarrow{P}^{\mathrm{ES}*}_{\mathrm{v,t}}(\mathrm{k}+1)$ and $\lambda^{\mathrm{LEM}}_{\mathrm{t,i}}(\mathrm{k})$ from the solution.

7. Update $\lambda^{\mathrm{LEM}*}_{\mathrm{t,i}}(\mathrm{k}+1)=\lambda^{\mathrm{LEM}}_{\mathrm{t,i}}(\mathrm{k})+\rho\left(\overleftrightarrow{P}^{\mathrm{ES}*}_{\mathrm{v,t}}(k)-\left(\vec{P}^{\mathrm{ES}*}_{\mathrm{t,v}}(k)-\overleftarrow{P}^{\mathrm{ES}*}_{\mathrm{t,v}}(k)\right)\right)$

8. Terminate the algorithm if $\left|\lambda^{\mathrm{LEM}*}_{\mathrm{t,i}}(\mathrm{k})-\lambda^{\mathrm{LEM}*}_{\mathrm{t,i}}(\mathrm{k}+1)\right|/\lambda^{\mathrm{LEM}*}_{\mathrm{t,i}}(\mathrm{k})\le\varepsilon$. Otherwise, return to line 2

At first step of the algorithm, the MCP of LEM ($\lambda^{\mathrm{LEM}*}_{\mathrm{t,i}}$) is acquired from the dual variable value of the Eq. (36), wherein the sign "$*$" stands for the value of the this dual decision variable, and a random value is denoted to $\vec{P}^{\mathrm{ES}*}_{\mathrm{v,t}}$, which is the amount of energy that LEM operator wants to exchange with the IEVSDGs. The sign "$*$" stands for the value of the this dual decision variable. At the second step, IEVSDGs' objective function (first level) is minimized, while adding a penalty term to the objective function. Here, $\overleftrightarrow{P}^{\mathrm{ES}*}_{\mathrm{v,t}}$ is parametric value of energy exchange which is provided by the LEM. In other word, the penalty term is applied when the energy transaction variables between first and second levels are different. As can be observed, this term is quadratic, which allow the small variations tolerable and pushes the algorithm towards the point of equilibrium in each iteration, which is the basis for the ADMM method [49]. At the third step, the optimal energy change parametric value of the first and second levels are updated after solving the first level problem. The second level and third level problems form a bi-level model, which is merged into a single-level problem through the KKT conditions [48]. This new merged problem is designated by $OF_{2\&3}$. As it was mentioned, OF_1 and $OF_{1\&3}$ form the main bi-level problem in the ADMM. At the fifth step, the same quadratic penalty term of second step is added to $OF_{1\&2}$ and the optimization problem is solved. At the sixth and seventh steps, the MCP of the LEM and energy transaction parametric values are updated, respectively. Eventually, if the MCP of the LEM converges to certain value in consecutive iterations, the algorithm is stopped at the eighths step. Otherwise, the loop is reiterated from the second step.

4. Numerical simulations and results

In the current study, the vehicles were clustered into 9 EVFs with similar stochastic behavioural patterns using the k-means clustering method, and their data was obtained from [50,51]. These clusters form the IEVSDGs together with SDGs, which are scattered across the distribution system. Fig. 3 depicts the overall topology of these IEVSDGs, systems, connection and equipment sites. As can be observed the WEM is modelled through a standard IEEE 24-bus TN [47], while LEM (operated by Disco) is established by a standard 69-bus ADS [52]. The WEM involves 12 Gencos, and the LEM includes 10 DG. Additionally, the ADS is linked to TN through the 20th node. Fig. 4 illustrates the arrival/departure time data distribution of each EVFs, while the empirical probability distribution function for their daily travelled miles is captured in Fig. 5. These distributions are deployed to generate the stochastic scenarios associated with each EVF. The data on EVs was obtained from [53]. Furthermore, all these data are included in the online repository [54]. In this regard, 10000 scenarios were generated by random sampling from these distributions, which were then reduced to 10 most probable cases by forward scenario reduction method [55]. The expected value of the solar energy production and considered variation interval of RO is illustrated in Fig. 6. To illustrate the impact of IEVSDGs in various markets by the proposed tri-level optimization framework, the following case studies (CS) are devised:

CS1: In this case, no control strategy is applied to vehicles and their battery is charged from the moment they park until full charge. (Also known as dumb charging.)

CS2: In this model, a smart charging strategy is exerted on EVFs. In the smart charging strategy, the charge/discharge powers of the EVFs

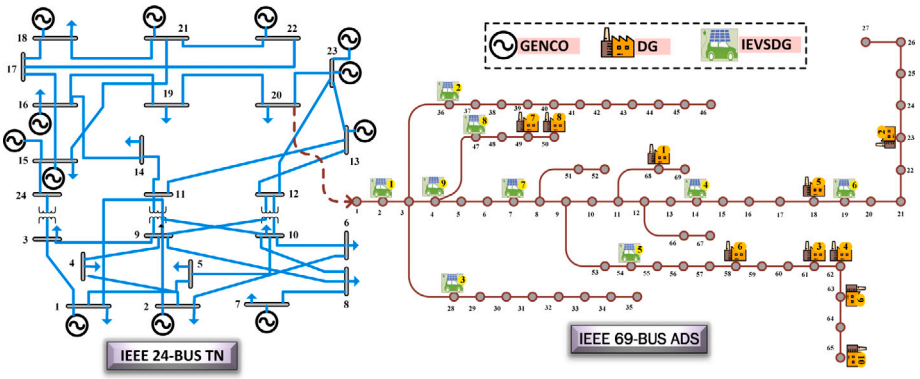

Fig. 3. The topology and connections of different system, equipment and markets.

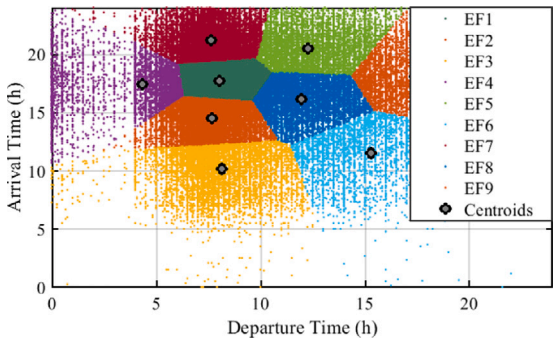

Fig. 4. EVFs' arrival/departure time points of EVFs.

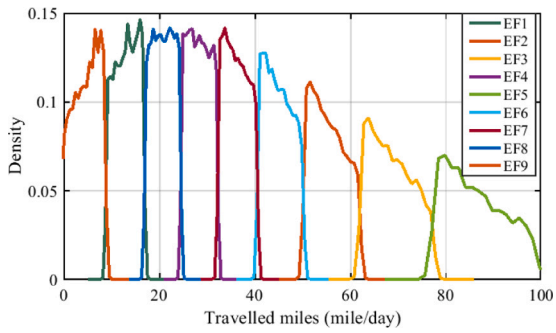

Fig. 5. Distribution of EVFs' daily travelled miles.

are the decision variable that are obtained from solving the proposed tri-level stochastic model

CS3: In this case, the RO framework is included in CS2 to handle SDGs uncertainties in RO-SP framework. (considering $\Gamma^{RO} = 1$)

In mathematical terms, the proposed problem consists of two mixed integer quadratic programming (MIQP) optimization models in main body of the ADMM. The first one is the IEVSDGs' problem that forms the first level, while the second problem was formed from the merger of the second and third levels by the KKT conditions. These MIQPs were solved on an Intel(R) Core (TM) i5-8250U CPU @ 1.60 GHz (4 CPUs), RAM 8 GB system in 24 min, using standard CPLEX solver.

The hourly SOC scheduling (concerns the first level) of the EVFs is summarized in Fig. 7 throughout various cases. As can be noticed, in CS1 the SOC of EVFs demonstrates a steady and sharp increase in hours 11 to 19, which corresponds to the time interval that most EVFs reach the parking lot (see [41]), and they immediately start the charging process. However, in CS2 the optimal scheduling has shifted the charging process (see the slope of the curves) to hours 13–11 that is associated with the off-peak interval in both LEM and WEM. This shift in charging scheduling is even more predominant in CS3. Evidently, the reason is that the RO framework enforces the problem to take conservative steps regarding solar energy production. Therefore, a further quantity of the charging load is shifted back to off-peak periods to profit from higher market prices and compensate solar power shortage.

The hourly optimal power dispatch scheduling of DGs (owned by Disco and concerns the second level) is plotted in Tables 2–4 regarding various cases. The most notable outcome is that when EVs are charged without any control in CS1, the peak EV charging demand accumulates on the already existing residential load. The result is that a huge surge in demand activates the interruptible loads (101.82 MWh in total) as a measure against security constraints' violation. Furthermore, Expensive DGs (No: 2,3,8,10) are operating with high power dispatch. On the other hand, in CS2 a large portion of the charging demand is moved to off-peak intervals, which is in line with SOC observations in Fig. 7. Overall, in this case, the interrupted load value is zero. When compared with CS1, the overall DG production is dropped by 50.71%, the losses reduced by 25.02% and power imported from WEM is increased by 11.05%, which is because cheaper energy is purchased during off-peak intervals. The robust formulation of CS3, has engendered a conservative scheduling program. In this case, the overall DG production has surged by 22.66% compared to CS2, while the WEM provides 8.4% higher portion of demand, which is an attempt to decrease the involved risks in SDGs' underproduction contingencies (see Fig. 8).

The MCP of the LEM is demonstrated by Fig. 9. As can be seen, CS1 imposes the highest MCP value at the local level. The reason is that not only this case has the highest DG production level, but also the expensive interruptible loads have augmented the MCP dramatically. According to the experimental outcomes, the MCP of this case is a staggering 180% higher than that of the CS2, which shows the capabilities of the EVFs as a local price-maker. Furthermore, CS3 has a 4.06% higher local MCP since the solar production risks are included in the RO framework. Another notable phenomenon is that the MCP of CS1 is rather low during the off-peak intervals, which is due to the fact that EVs demand is not shifted to these periods that would have increased the MCP. This observation also emphasizes the huge gap between the peak and off-peak periods when EV charging is uncoordinated.

At the third level, the energy procurement strategy of the WEM throughout different cases is depicted in Fig. 10 for the most expensive generation unit (Genco4), and in Fig. 11 for the cheapest generation unit (Genco11) of the standard 24-bus TN. In Fig. 10, it can be observed, that CS1 enforces the expensive Genco4 to operate with higher production to compensate the demand peak imposed by the

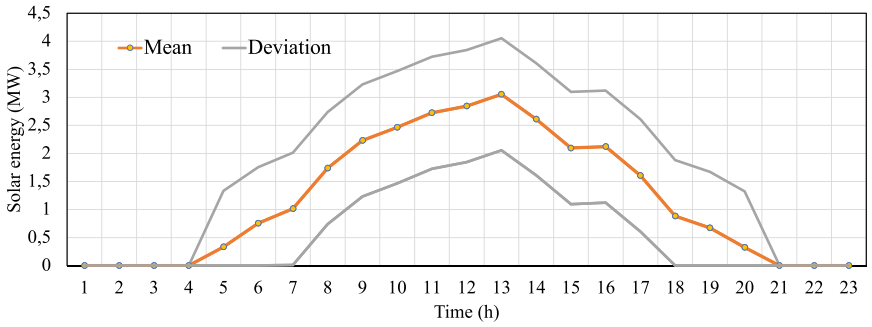

Fig. 6. The solar energy production profile of RO.

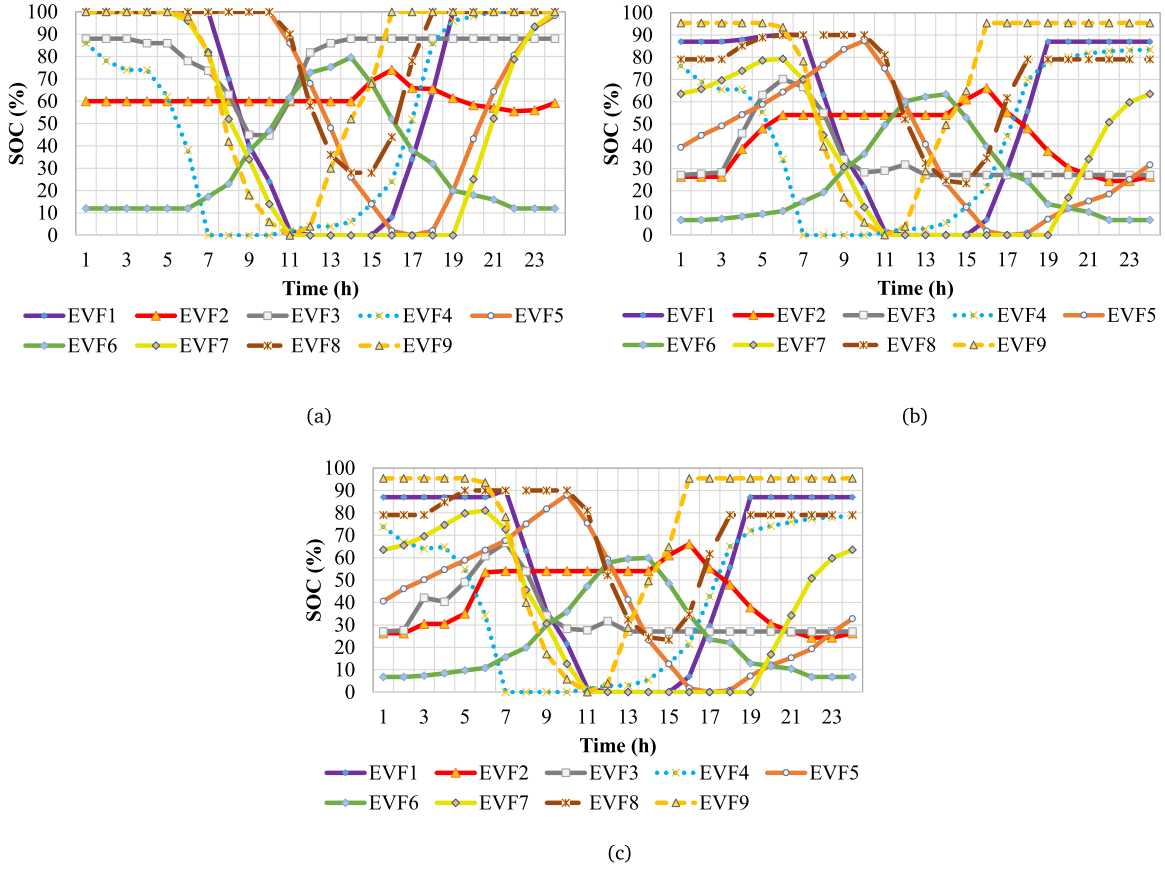

Fig. 7. The SOC of EVFs: (a) **CS1** (b) **CS2** (c) **CS3**.

uncoordinated electric vehicles in the IEVSDG level (first level). In particular, the production of this expensive units is diminished by 176 MWh (23.8%). However, it is noted that CS3 imposes 65.5 MWh more demand in this expensive unit compared to CS2, which is imposed to mitigate the conservative estimates in SDG production. Fig. 11 shows that the cheap unit of Genco11 has 292.7 MWh (4.4%)more production in CS2 compared to CS1, which is due to the fact that the smart charging has successfully shifted the EVs charging demand to off-peak hours to take advantage of this cheap Genco. It can be noted that after hour 11 this unit has the highest production regardless of the case study, since it is a cheap production unit. It is noted that in CS3, the increase in the production of this units is still 247 MWh more compared to CS1, while it is 45 MWh lower than CS2. The reason is that smart charging strategy shifts the demand to off-peak hours. However, the Conservative operation state of CS3 slightly limits the system flexibility by robust estimation of SDG production.

In summation, CS1 enforces the expensive Gencos to operate with expensive piecewise blocks. For instance, cheap production units, i.e., Genco 11 & 12 have 3.4% lower production regarding CS2, while expensive units, i.e., Genco 1–7 have a 3.03% higher production rate. On the other hand, large units i.e., Genco 8–10 are activated ceaselessly in all cases as they support the base demand. CS3 has imported even a higher portion of the load through cheaper units (1.33% higher than CS2) as it relies heavily on the market to mitigate the possible lack of SDGs production. The MCP of the WEM is plotted in Fig. 12. The results further confirm the previous statements on the Genco scheduling at WEM level. Accordingly, CS1 has the highest MCP for the WEM since a large quantity of the demand is procured by high-cost Gencos. Overall, the MCP of the WEM is 0.86% lower in CS2, which testifies the price-maker qualities of the IEVSDG at WEM level. Additionally, the MCP is 0.50% lower in CS3, which is still marginally higher than the price in CS2. Nevertheless, the results are scheduled for conservative SDG

Table 2
The power demand schedule of the local energy market in CS1.

	DG1	DG2	DG3	DG4	DG5	DG6	DG7	DG8	DG9	DG10	PV	WEM	IL	loss	EVF	DSL
1	0	3.09086	0.5	0.75	0.801504	0.5	0	0.3	1	1	0	41.80185	0	−1.32858	−6.6072	41.05843
2	0	3.29086	0	0	1.116773	0	0	0	0.5	0.5	0	34.62777	0	−1.04274	0	38.99266
3	0	3.49086	0	0	0.75	0	0	0	0	0	0	26.91149	0	−0.5057	0	30.64665
4	0.35	3.69086	0	0	0.75	0	0	0	0	0	0	19.33888	0	−0.16321	0	23.96653
5	0.7	3.89086	0	0	0.75	0	0	0	0	0	2.992896	16.19065	0	−0.16636	0	24.35804
6	1.05	4.09086	0	0	0.75	0	0	0	0	0	6.790896	12.4633	0	−0.18269	0	24.96236
7	1.4	4.29086	0	0	1.25	0	0	0	0.3	0	9.115218	25.54711	0	−0.51954	−6.753	34.63066
8	1.75	4.49086	0	0	1.75	0.5	0	0	0.8	0	15.65064	35.53615	0	−1.21219	−13.6255	45.63998
9	2.1	4.69086	0.8	0	2.25	1	0.6	0	1.3	0.5	20.079	35.92172	0	−1.45121	−19.8579	47.93242
10	2.45	4.89086	0.870489	0	2.75	1.5	1.2	0.6	1.8	0.474067	22.1985	40.4648	0	−1.17657	−25.4009	52.62125
11	2.8	5.09086	1.670489	0	3.25	2	1.8	1.2	2.3	0.974067	24.52284	60.55237	0	−1.21038	−51.5782	53.37209
12	3.15	5.29086	2.470489	0	3.75	2.5	2.4	1.8	2.8	1.474067	25.5852	52.85845	0	−0.58676	−54.1266	49.36567
13	3.5	5.09086	2.4	0	3.5	2.5	1.8	1.2	2.3	0.974067	27.48852	34.0043	0	−0.73115	−35.6896	48.33702
14	3.85	5.2	3.2	0	4	3	1.2	0.6	2	1.474067	23.49468	24.5078	0	−1.26095	−25.1716	46.09402
15	4.2	5.4	4	0	4.5	3.5	1.60426	0.3	2.5	1.974067	18.86886	32.57778	0	−1.46434	−24.5855	53.37509
16	4.55	5.6	4.8	0	5	4	2.20426	0.775121	3	2.474067	19.08846	60.50625	0	−3.32774	−52.6859	55.9845
17	4.9	5.8	5.6	0	5.5	4.5	1.754109	0.3	3.5	2.974067	14.46032	80.62664	0	−5.90372	−73.4336	50.57781
18	5.25	6	6.4	0	6	5	2.354109	0.9	4	3.474067	7.943094	85.66313	4.107319	−7.42863	−76.7932	52.86987
19	5.6	5.8	7.2	0	6.5	5.5	1.8	1.5	4.5	3.974067	6.058602	93.30042	0	−4.44825	−81.2128	56.072
20	5.95	6	8	0	7	6	2.4	2.1	5	4.474067	2.911518	70.07677	35.82671	−5.75394	−91.7779	58.20719
21	6	6	8	0	7	6	1.8	1.797296	5	4.504933	0	64.4502	42.21675	−6.41677	−87.9402	58.41225
22	6	6	8	0	7	6	1.2	1.197296	5	4.004933	0	64.8562	23.78298	−6.12794	−74.0747	52.83878
23	5.65	5.8	7.2	0	6.5	5.5	0.6	0.597296	4.5	3.504933	0	63.40079	0	−5.01199	−47.4142	50.82678
24	5.3	5.6	6.4	0	6	5	0	0	4	3.004933	0	42.19344	0	−4.55048	−25.4862	47.46166

Table 3
The power demand schedule of the local energy market in CS2.

	DG1	DG2	DG3	DG4	DG5	DG6	DG7	DG8	DG9	DG10	PV	WEM	IL	loss	EVF	DSL
1	0	4.75444	0.5	0.75	0.763188	0.5	0	0.3	5	0.4	0	49.55426	0	−2.14602	−18.5674	41.05843
2	0	4.55444	0	0	1.263188	0	0	0	4.672763	0.5	0	52.36613	0	−2.09465	−22.2692	38.99266
3	0	4.35444	0	0	1.035427	0	0	0	4.172763	0	0	51.00905	0	−1.90465	−28.0204	30.64665
4	0	4.15444	0	0	0.75	0	0	0	3.672763	0	0	145.5089	0	−2.03553	−128.084	23.96653
5	0	3.95444	0	0	0.75	0	0	0	3.604	0	2.992896	128.0415	0	−1.97288	−113.012	24.35804
6	0	3.75444	0	0	0.75	0	0	0	3.842498	0	6.790896	99.05541	0	−2.01577	−87.2151	24.96236
7	0	3.55444	0	0	1.25	0	0	0	4.342498	0.430206	9.115218	50.42237	0	−2.09414	−32.3899	34.63066
8	0	3.574965	0	0	1.75	0	0	0	4.842498	0.930206	15.65064	49.01129	0	−2.42195	−27.6977	45.63998
9	0	3.774965	0	0	2.25	0	0	0.3	4.725917	1	20.079	43.3932	0	−2.51164	−25.079	47.93242
10	0	3.974965	0	0	1.75	0	0.567746	0.9	4.225917	0.5	22.1985	35.93691	0	−1.88571	−15.5471	52.62125
11	0	4.032011	0	0	1.25	0	1.167746	0.6	3.725917	0	24.52284	29.39585	0	−1.72706	−9.59521	53.37209
12	0	3.832011	0	0	0.75	0	0.567746	0	3.225917	0	25.5852	23.94075	0	−1.66294	−6.87301	49.36567
13	0	3.833802	0	0	0.75	0	0	0	3.115376	0	27.48852	21.33335	0	−1.66669	−6.51735	48.33702
14	0	4.033802	0	0	0.75	0	0.59422	0	3.615376	0	23.49468	26.56531	0	−1.54127	−11.4181	46.09402
15	0	4.233802	0	0	0.878018	0	1.19422	0.6	4.115376	0	18.86886	33.46551	0	−1.80791	−8.17279	53.37509
16	0	4.433802	0	0	0.993486	0	1.79422	0.935954	4.615376	0	19.08846	46.93365	0	−1.83204	−20.9784	55.9845
17	0.35	4.633802	0	0	0.75	0	1.19422	0.335954	4.350019	0	14.46032	39.97413	0	−1.64993	−13.8207	50.57781
18	0.7	4.833802	0	0	1.25	0	1.79422	0	4.850019	0	7.943094	38.71987	0	−1.69552	−5.52561	52.86987
19	1.05	5.033802	0	0	1.75	0	2.333455	0.555646	5	0	6.058602	42.81184	0	−1.74164	−6.77971	56.072
20	0.7	5.233802	0	0	1.756128	0	2.4	1.155646	5	0	2.911518	45.32227	0	−1.86389	−4.40828	58.20719
21	0.35	5.433802	0	0	1.941217	0	1.8	1.707521	5	0	0	44.86608	0	−1.89311	−0.79326	58.41225
22	0	5.633802	0	0	1.441217	0	1.2	1.107521	4.5	0	0	43.12295	0	−1.78406	−2.38265	52.83878
23	0	5.833802	0	0	1.941217	0	0.6	0.507521	5	0.5	0	49.68311	0	−2.16744	−11.0714	50.82678
24	0	5.754063	0	0	2.441217	0	0	0	5	0.4	0	52.18961	0	−2.46536	−15.8579	47.46166

production values. These values might seem trivial. However, considering the large scale of the WEM it is only fair for players to be able to influence market price with minute values, which is also the case in other markets that have different products rather than electricity. The voltage profile of 69-bus ADS at peak time (hour 21) is plotted for all buses in Fig. 13. In terms of deviation from the base voltage, CS1 demonstrates the lowest root mean square (RMS) of deviations, as the RMS of deviations from the base is 0.3448 kV (2.72%). This might look uncanny, as this case has the most destructive impact of uncoordinated charging. However, a huge amount of interrupted load lies under the facade of this rather desirable profile. The RMS of deviations from the base value in CS2 and C3 are 0.5797 kv (4.57%) and 0.5648 kV (4.46%), respectively. The reason for this improved profile in CS3 is that the possible SDG shortage contingencies are considered in RO framework, which enforces the algorithm to shift a higher amount of EV load to off-peak periods. Nevertheless, this action leads to higher local LMP in CS3. The maximum voltage value at CS2 & cs3 is 12.66 kv. However, in CS1, the maximum voltage value of 13.92 kv was noted, which is equal to the highest bound of voltage variable. This outcome is due to the high load shedding in this CS1, which might also lead to voltage instability due to the uncontrolled charging demand of the EVFs.

The optimal solution values for important decision variables, such as the objectives of various levels are summarized in Table 5, which substantiates the previously mentioned hypothesis. As can be noticed, the uncoordinated charging strategy in CS1 gives rise to the highest operational cost at all levels, while the value of power loss and interruptible loads are unacceptably high, which is due to the uncoodinated charging mode of CS1. The most notable discrepancy between CS1 and CS2 is the cost of energy and amount of energy that is purchased from the WEM by Disco. As can be observed higher energy is imported with lower cost in coordinated charging mode. The reason is that a large

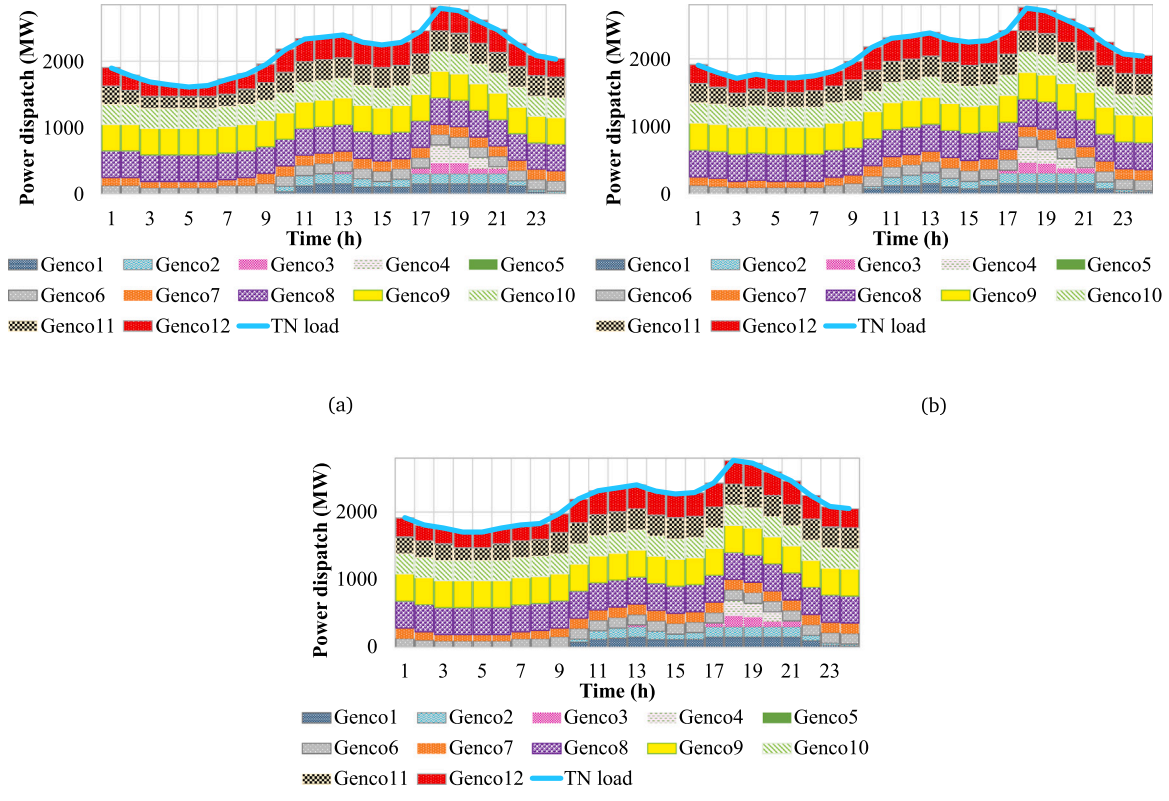

Fig. 8. The power schedule of the WEM: (a) **CS1** (b) **CS2** (c) **CS3**.

Table 4
The power demand schedule of the local energy market in CS3.

	DG1	DG2	DG3	DG4	DG5	DG6	DG7	DG8	DG9	DG10	PV	WEM	IL	loss	EVF	DSL
1	0	4.972808	0.5	0.75	0.75	0.5	0	0.3	5	0.4	0	49.54375	0	−2.15154	−18.7566	41.05843
2	0	4.910826	0	0	1.25	0	0	0	4.745791	0.465778	0	52.30601	0	−2.10603	−22.5797	38.99266
3	0	5.110826	0	0	0.900789	0	0	0	4.245791	0	0	92.72576	0	−1.90659	−70.4299	30.64665
4	0.3	5.310826	0	0	0.75	0	0	0	3.745791	0	0	67.026	0	−2.12852	−51.0376	23.96653
5	0.3	5.510826	0	0	0.75	0	0	0	3.73363	0	0	96.58478	0	−2.10149	−80.4197	24.35804
6	0.3	5.710826	0	0	0.75	0	0	0	3.874574	0	0	133.6932	0	−2.11078	−117.255	24.96236
7	0.65	5.910826	0	0	1.25	0	0	0	4.374574	0.4	0	98.97066	0	−2.1687	−74.7567	34.63066
8	0.3	6	0	0	1.75	0	0	0	4.874574	0.9	2.15064	51.76833	0	−2.42138	−19.6822	45.63998
9	0.65	6	0	0	2.25	0	0	0.334896	5	0.905408	6.579	53.66149	0	−2.60576	−24.8426	47.93242
10	1	6	0	0	2.75	0	0.6	0.934896	5	0.487867	8.6985	49.0509	0	−2.23643	−19.6645	52.62125
11	1.35	6	0.8	0	2.25	0.5	0.6	1.2	5	0.5	11.02284	29.39585	0	−1.11726	−4.12934	53.37209
12	1	6	0	0	1.75	0	0	0.6	4.5	0	12.0852	34.84727	0	−1.5121	−9.9047	49.36567
13	0.65	6	0	0	1.25	0	0.5	0	4	0	13.98852	29.55216	0	−1.54139	−6.06227	48.33702
14	0.3	6	0	0	0.75	0	0.649541	0	4	0	9.99468	35.60492	0	−1.60395	−9.60117	46.09402
15	0.65	6	0	0	1.06883	0	1.249541	0.6	4.5	0	5.36886	42.97662	0	−1.86831	−7.17045	53.37509
16	1	6	0	0	1.137002	0	1.849541	0.93506	5	0	5.58846	56.27443	0	−1.89385	−19.9061	55.9845
17	1.35	6	0	0	1.230943	0	1.249541	0.33506	4.5	0	0.960318	48.52564	0	−1.60933	−11.9644	50.57781
18	1.7	6	0	0	1.730943	0	1.820068	0	5	0	0	42.5562	0	−1.61383	−4.3235	52.86987
19	2.05	6	0	0	2.230943	0	2.343994	0.56156	5	0	0	45.98384	0	−1.66947	−6.42887	56.072
20	1.7	6	0	0	2.116064	0	2.4	1.16156	5	0	0	46.63323	0	−1.80053	−5.00313	58.20719
21	1.35	6	0	0	2.278651	0	1.8	1.703179	5	0	0	44.03932	0	−1.80363	−1.95527	58.41225
22	1	6	0	0	1.778651	0	1.2	1.103179	4.5	0	0	43.91243	0	−1.78318	−4.8723	52.83878
23	0.65	6	0	0	2.278651	0	0.6	0.503179	5	0.5	0	50.61623	0	−2.23723	−13.0841	50.82678
24	0.3	5.8	0	0	2.778651	0	0	0	5	0	0	51.37495	0	−2.36224	−15.4297	47.46166

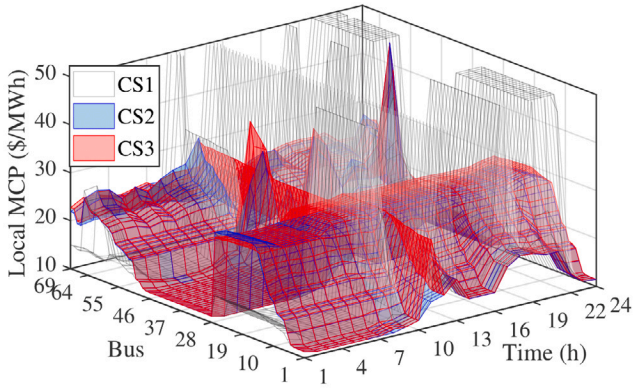

Fig. 9. The MCP of the LEM (IEEE-69 bus).

quantity of the charging load is moved to off-peak hours that provide cheaper energy. In particular, this effect was proven by Figs. 10 and 11.

Moreover, the cost of DG operation is remarkably lower since the load is shifted and DGs are not obliged to operate in high-cost modes. In general, when the RO framework is deployed (CS3), the costs are slightly higher as possible SDG production shortages are modelled conservatively. Furthermore, the EVFs' battery erosion cost for supporting the grid is nearly 88% higher in CS3 since the SDG production estimates are conservative and the EVFs take on more pressure the compensate for this production shortage.The battery degradation cost is zero in CS1, as in EVFs do not provide any service in the uncoordinated charging mode. In order to observe the iterative convergence of the ADMM algorithm the value of IEVSDG objective function in each integration is remonstrated in Fig. 14. As it can be noted, the cost value shows a very fast decline in the first few iterations as the initial values are given in random. However, the difference between two consecutive iterations were negligibly small after the 30th iteration, which was a sign that the ADMM had converged to the optimal solution

It is imperative to observe the impact of uncertainty in the third level as it has a essential role in market clearing process. In this regard, two wind farms with production capacity of 100 MW were installed on the 5th and 17th nodes of the TN. Fig. 15 shows the MCP of the WEM for different Γ values. Based on the results, the higher values of Γ leads to a marginally higher energy price. In particular, the robust solutions shows 5.11% higher MCP when the RO is deployed. It should be noted that this higher price ensures a more robust and reliable operation for the TN. Eventually it is noteworthy to sum up the main highlights in the obtained results from this study. The results show that using the proposed three-level model leads to 0.86% reduction in the wholesale market price and 57% in LEM price. Therefore, it testifies the benefits of combining these two market models. Likewise, in the study [29] a similar reduction in the local market price was reported, while the retailer was a price-taker in the WEM. On the other hand, [28] had reported a similar amount of reduction (0.5%–0.9%) in the WEM price. Nevertheless, this study ignored the impact of small-scale player such as IEVSDGs on the LEM clearing price. Additionally, some studies such as [39] have ignored the possibility of using EVs as flexible loads through smart charging, and the EVS are modelled as constant load. To this end, the outcomes of this study illustrated that through the proposed model the peak demand could be shaved dramatically, which ultimately led to elimination of 105 MWh of total lead interruptions that occur due to security-induced reason, and overloading of the ADS.

5. Conclusion

This study investigated a tri-level strategic price-maker optimization framework for integrated electric vehicle fleets and solar distributed generations (IEVSDG) to participate in the local electricity market (LEM was operated by Disco), considering that Disco itself is an strategic price-maker in the wholesale electricity market (WEM). In the proposed model, the IEVSDGs formed the first level, the Disco operator was the second level, while the WEM operator was integrated to the third level. To solve the tri-level problem, the second and third levels were unified in a single problem by utilizing KKT conditions. Ultimately, the equilibrium point between the first level and this conjoined problem was achieved through the alternating direction method of multipliers. The study investigated various coordinated, smart and robust charging strategies and reached the following conclusive points:

1. By smart charging scheduling strategy (CS2), the IEVSDGs can become a price-maker at LEM as marginal electricity price was reduced by 180% compared to dumb charging strategy (CS1). Although in the real-word circumstances all vehicles might not be charged uncoordinatedly, their destructive impact would still be significant at the local market level.
2. Through the liaison of the Disco, IEVSDGs can also be a price-maker at the WEM level by reducing the wholesale market price by 0.86%.
3. The reduction in the market clearing price at both the local and wholesale market levels prove that IEVSDGs can effectively deploy the proposed tri-level model the improve its market strategy at deeper levels.

Table 5
Important decision variables in different cases.

	CS1	CS2	CS3
First level objective ($)	159 891.9	5918.752	9035.00
Second level objective ($)	84 613.35	23 247.6	26 373.89
Third level objective ($)	410 217.2	410 333.2	410 349.4
Total interrupted load (kWh)	105.933	0	0
Total power losses (kWh)	61.9718	46.581	46.353
Total Energy import of LEM from WEM (kWh)	1118.37	1242.623	1347.623
Total Genco generation (kWh)	51 482.89	51 607.14	51 712.14
Total DG generation (kWh)	563.979	278.139	340.906
Total SDG power generation (kWh)	247.249	247.249	76.437
Total energy purchase of LEM in WEM ($)	17 151.73	16 193.80	17 686.55
Total load interruption cost ($)	52 966.88	0	0
Total unit commitment cost ($)	14 494.73	7053.79	8687.33
Total battery degradation cost ($)	0	319.721	601.32

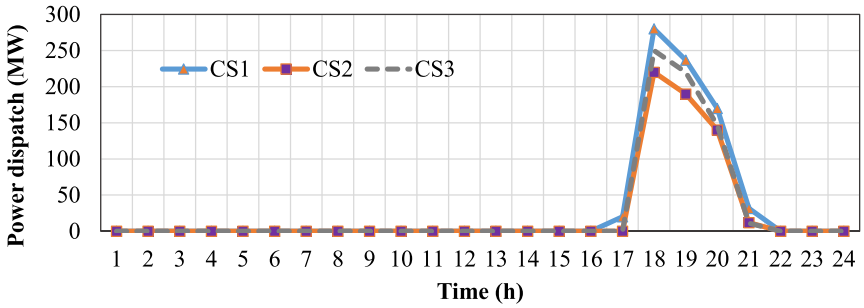

Fig. 10. The energy dispatch schedule of Genco4.

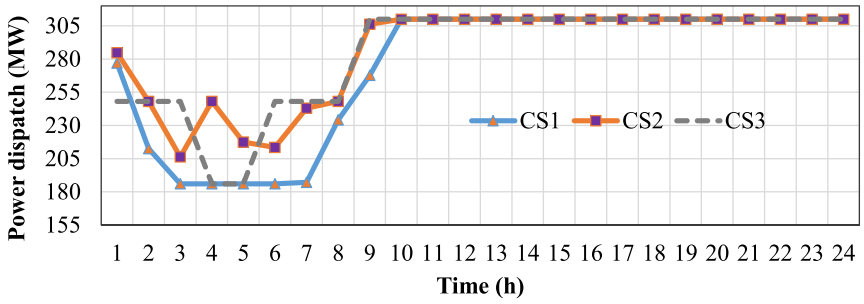

Fig. 11. The energy dispatch schedule of Genco11.

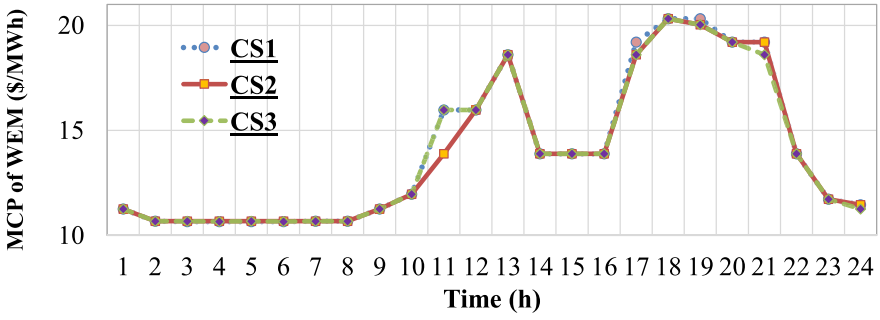

Fig. 12. The MCP of the WEM.

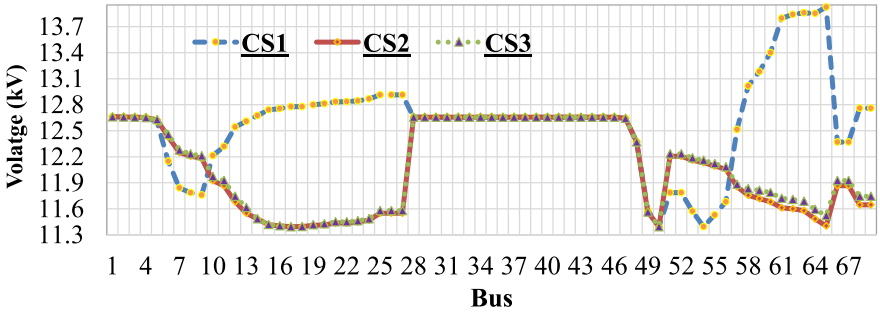

Fig. 13. The Voltage profile of 69-bus ADS.

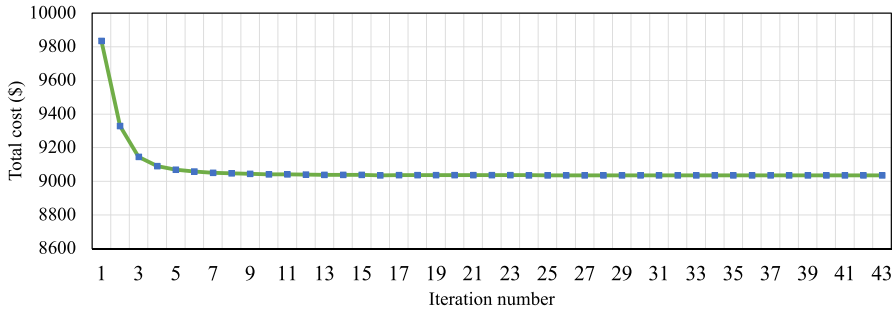

Fig. 14. The convergence of the total cost of IEVSDG in ADMM.

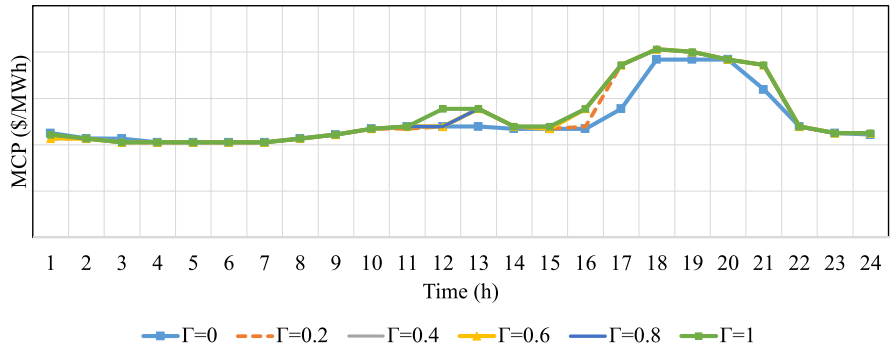

Fig. 15. The sensitivity of the MCP of WEM for different robustness levels in wind production uncertainty.

4. Dumb charging strategy (CS1) marks the highest operational cost values for all market levels. Furthermore, power losses, interrupted loads, local and wholesale market prices are dramatically high.
5. Although the operational cost in the RO framework (CS3) is slightly higher than the deterministic case (CS2), it provides a reliable operation scheduling since perfect forecasting is highly unexpected.

CRediT authorship contribution statement

Saeed Zeynali: Conceptualization, Methodology, Software, Writing – original draft, Data curation, Visualization. **Nima Nasiri:** Software, Methodology, Writing – original draft, Visualization. **Sajad Najafi Ravadanegh:** Formal analysis, Supervision, Validation, Investigation, Project administration. **Sylvain Kubler:** Formal analysis, Supervision, Validation, Investigation, Project administration. **Yves Le Traon:** Supervision, Validation, Investigation.

Declaration of competing interest

The authors declare that they have no known competing financial interests or personal relationships that could have appeared to influence the work reported in this paper.

Data availability

Data will be made available on request.

Acknowledgement

This work was supported by the Luxembourg National Research Fund (FNR) LightGridSEED Project, ref. C21/IS/16215802/LightGrid SEED. For the purpose of open access, and in fulfilment of the obligations arising from the grant agreement , the author has applied a Creative Commons Attribution 4.0 International (CC BY 4.0) license to any Author Accepted Manuscript version arising from this submission.

Appendix A. Mathematical program with equilibrium constraints (MPEC)

In bi-level optimization problems that the lower level is a convex problem, the KKT conditions can effectively convert the model into a single-level optimization problem. In this study, the third level problem is the wholesale electricity market optimization to maximize the social welfare, which is a convex model. Therefore, we replaced this model by its KKT conditions to convert the second and third levels into a single problem. The KKT conditions of the wholesale electricity market are as follows:

A.1. Stationary conditions

The lagrangian function of the proposed problem can be defined by Eq. (A.1), where x represents the vector of decision variables, while $f(x)$, $h(x)$ and $g(x)$ are the objective function, equality constraints and inequality constraints. The stationary conditions state that the derivatives the lagrangian function over each variable must be equal to zero, which is developed as follows:

$$L^{EN} = f(x) + \lambda^T h(x) + \mu^T g(x) \tag{A.1}$$

$$\frac{\partial L^{\mathrm{EN}}}{\partial P^{\mathrm{G}}_{\mathrm{g,t}}} = -\lambda^{\mathrm{WEM}}_{\mathrm{b,t}} + \overline{\mu^{1}_{\mathrm{g,t}}} - \underline{\mu^{1}_{\mathrm{g,t}}} + \mu^{3}_{\mathrm{g,t}}|_{t>1} - \mu^{3}_{\mathrm{g,t+1}}|_{\mathrm{t>1}} + \mu^{4}_{\mathrm{g,t}}|_{t=1} - \mu^{5}_{\mathrm{g,t}}|_{\mathrm{t>1}} + \overline{\mu^{5}_{\mathrm{g,t+1}}}|_{\mathrm{t>1}} + \mu^{6}_{\mathrm{g,t}}|_{\mathrm{t=1}} + \lambda^{1}_{\mathrm{g,t}} = 0 \forall \mathrm{g} \in A^{\mathrm{g}}_{\mathrm{b}}, \forall \mathrm{b}, \forall \mathrm{t} \tag{A.2}$$

$$\frac{\partial L^{\mathrm{EN}}}{\partial \rho^{\mathrm{G}}_{\mathrm{g,m,t}}} = C^{\mathrm{G}}_{\mathrm{g,m}} + \overline{\mu^{2}_{\mathrm{g,m,t}}} - \underline{\mu^{2}_{\mathrm{g,m,t}}} - \lambda^{1}_{\mathrm{g,t}} = 0 \forall \mathrm{g}, \forall \mathrm{m}, \forall \mathrm{t} \tag{A.3}$$

$$\frac{\partial L^{\mathrm{EN}}}{\partial p^{\mathrm{Dsc}}_{\mathrm{t}}} = -C^{\mathrm{Dsc}}_{\mathrm{t}} + \lambda^{\mathrm{WEM}}_{\mathrm{b,t}} + \overline{\mu^{7}_{\mathrm{t}}} - \underline{\mu^{7}_{\mathrm{t}}} = 0 \forall \mathrm{t} \tag{A.4}$$

$$\frac{\partial L^{\mathrm{WT}}}{\partial P^{\mathrm{WT}}_{\mathrm{w,t}}} = -\lambda^{\mathrm{WEM}}_{\mathrm{b,t}} + \overline{\mu^{8}_{\mathrm{w,t}}} - \underline{\mu^{8}_{\mathrm{w,t}}} = 0 \forall \mathrm{w}, \forall \mathrm{t} \tag{A.5}$$

$$\frac{\partial L^{\mathrm{EN}}}{\partial \delta_{\mathrm{b,t}}} = \sum_{\mathrm{b'} \in Tr} B_{\mathrm{b,b'}} (\lambda^{\mathrm{WEM}}_{\mathrm{b,t}} - \lambda^{\mathrm{WEM}}_{\mathrm{b',t}}) + \sum_{\mathrm{b'} \in Tr} B_{\mathrm{b,b'}} (\overline{v_{\mathrm{b,b',t}}} - \overline{v_{\mathrm{b',b,t}}}) + \sum_{\mathrm{b'} \in Tr} B_{\mathrm{b,b'}} (\underline{v_{\mathrm{b',b,t}}} - \underline{v_{\mathrm{b,b',t}}}) + \overline{\xi_{\mathrm{b,t}}} - \underline{\xi_{\mathrm{b,t}}} + \xi^{1}_{b=1} = 0 \forall \mathrm{b}, \forall \mathrm{b'}, \forall \mathrm{t} \tag{A.6}$$

A.2. Primal, dual and complementary conditions

The primal, dual and complementary conditions can be summarized by following set of equations that state that outer multiplication of the primal and dual variables must be greater than zero.

$$0 \le P^{G}_{g,t} \perp \underline{\mu^{1}_{g,t}} \ge 0 \forall g, \forall t \tag{A.7}$$

$$0 \le (\overline{P^{G}_{g,t}} - P^{G}_{g,t}) \perp \overline{\mu^{1}_{g,t}} \ge 0 \forall g, \forall t \tag{A.8}$$

$$0 \le \rho^{G}_{g,m,t} \perp \underline{\mu^{2}_{g,m,t}} \ge 0 \forall g, \forall m, \forall t \tag{A.9}$$

$$0 \le (\overline{\rho_{g,m}} - \rho^{G}_{g,m,t}) \perp \overline{\mu^{2}_{g,m,t}} \ge 0 \forall g, \forall m, \forall t \tag{A.10}$$

$$0 \le (p^{Dsc}_{t} - \underline{p^{Dsc}_{t}}) \perp \underline{\mu^{7}_{t}} \ge 0 \forall t \tag{A.11}$$

$$0 \le (\overline{p^{Dsc}_{t}} - p^{Dsc}_{t}) \perp \overline{\mu^{7}_{t}} \ge 0 \forall t \tag{A.12}$$

$$0 \le (P^{WT}_{w,t} \perp \underline{\mu^{8}_{w,t}}) \ge 0 \forall w, \forall t \tag{A.13}$$

$$0 \le (\overline{P^{WT}_{w,t}} - P^{WT}_{w,t}) \perp \overline{\mu^{8}_{w,t}} \ge 0 \forall w, \forall t \tag{A.14}$$

$$0 \le (\overline{C_{b,b'}} + B_{b,b'}(\delta_{b,t} - \delta_{b',t})) \perp \underline{\upsilon_{b,b',t}} \ge 0 \forall b, \forall b', \forall t \tag{A.15}$$

$$0 \le (\overline{C_{b,b'}} - B_{b,b'}(\delta_{b,t} - \delta_{b',t})) \perp \overline{\upsilon_{b,b',t}} \ge 0 \forall b, \forall b', \forall t \tag{A.16}$$

$$0 \le (\pi - \delta_{b,t}) \perp \overline{\xi_{b,t}} \ge 0 \forall b, \forall t \tag{A.17}$$

$$0 \le (\pi + \delta_{b,t}) \perp \underline{\xi_{b,t}} \ge 0 \forall b, \forall t \tag{A.18}$$

The dual variable associated with the equality variables, such as Eqs. (39)–(40) and Eqs. (52) must be free in sign, which is defined as follows:

$$\lambda^{WEM}_{b,t} \forall b, t, \lambda^{1}_{g,t} \forall g, t, \xi^{1}_{b=1,t} \forall b, t \tag{A.19}$$

As can be observed, Eqs. (A.7)–(A.18) are nonlinear. To establish a MILP equivalent, the big-M method was used as defined in Eqs. (A.20)–(A.21), where M1 and M2 are very large numbers and u is a binary variable.

$$0 \le g_x \perp \mu \ge 0 \rightarrow g_x \ge 0, \mu \ge 0 \tag{A.20}$$

$$0 \le g_x \perp \mu \ge 0 \rightarrow g_x \ge 0, \mu \ge 0 \tag{A.21}$$

Appendix B. Linearization of $\lambda^{WEM}_{b,t} p^{Dsc}_{t}$ by the theory of strong duality

As can be observed from Eq. (18) of the main manuscript, the term $\lambda^{WEM}_{b,t} p^{Dsc}_{t}$ is a nonlinear term since both $\lambda^{WEM}_{b,t}$ and p^{Dsc}_{t} are continues decision variables. This term can be linearized by the theory of strong duality, which states that in optimal solutions point the value of the primal and dual optimization problems are equal, which is developed in Eq. (B.1) in Box I. Based on Eqs. (A.11) and (A.12), it can be derived that

$$0 \le (p^{Dsc}_{t} - \underline{p^{Dsc}_{t}}) \perp \underline{\mu^{7}_{t}} \ge 0 \rightarrow p^{Dsc}_{t} \underline{\mu^{7}_{t}} = \underline{p^{Dsc}_{t} \mu^{7}_{t}} \forall t \tag{B.2}$$

$$0 \le (\overline{p^{Dsc}_{t}} - p^{Dsc}_{t}) \perp \overline{\mu^{7}_{t}} \ge 0 \rightarrow p^{Dsc}_{t} \overline{\mu^{7}_{t}} = \overline{p^{Dsc}_{t} \mu^{7}_{t}} \forall t \tag{B.3}$$

In order to achieve a linear equivalent for $\lambda^{WEM}_{b,t} p^{Dsc}_{t}$, Eq. (A.4) is multiplied by p^{Dsc}_{t} as follows:

$$-p^{Dsc}_{t} C^{Dsc}_{t} + p^{Dsc}_{t} \lambda^{WEM}_{b,t} + p^{Dsc}_{t} \overline{\mu^{7}_{t}} - p^{Dsc}_{t} \underline{\mu^{7}_{t}} = 0 \forall t \tag{B.4}$$

$$p^{Dsc}_{t} C^{Dsc}_{t} = p^{Dsc}_{t} \lambda^{WEM}_{b,t} + p^{Dsc}_{t} \overline{\mu^{7}_{t}} - p^{Dsc}_{t} \underline{\mu^{7}_{t}} \quad \forall t \tag{B.5}$$

Eventually, the nonlinear term of $\lambda^{WEM}_{b,t} p^{Dsc}_{t}$ was replaced as given in Box II.

Appendix C. Battery degradation cost linearization

As can be observed, Eq. (11) is a nonlinear expression. To linearize the production of two continuous variables in battery erosion cost, the semi-integer linearization method is adopted from [41], as expressed by Eqs. (C.1)–(C.7). It should be noted that $\hbar^{a1}_{kl,v,s,t}$ and $\hbar^{a2}_{kl,v,s,t}$ are specially ordered semi-integer type two variables (SOS2) that have a auxiliary role in the linearization process. More details on this linearization method and SOS2 variables can be observed in [43].

$$y^{aux1}_{v,s,t} = 0.5\left(PD_{v,s,t} + MD_{v,s,t}\right) \forall v, s, t \tag{C.1}$$

$$y^{aux2}_{v,s,t} = 0.5\left(PD_{v,s,t} - MD_{v,s,t}\right) \forall v, s, t \tag{C.2}$$

$$dg^{NL}_{v,s,t} = PD_{v,s,t}.MD_{v,s,t} = \left(y^{aux1}_{v,s,t}\right)^2 - \left(y^{aux2}_{v,s,t}\right)^2 \tag{C.3}$$

$$\begin{aligned} FY^{aux1}_{v,s,t} &= \sum_{kl=1}^{KL} \hbar^{a1}_{kl,v,s,t} \left(\overline{y^{aux1}_{kl,v}}\right)^2, \\ FY^{aux2}_{v,s,t} &= \sum_{kl=1}^{KL} \hbar^{a2}_{kl,v,s,t} \left(\overline{y^{aux2}_{kl,v}}\right)^2 \forall v, s, t \end{aligned} \tag{C.4}$$

$$\begin{aligned} y^{aux1}_{v,s,t} &= \sum_{kl=1}^{KL} \hbar^{a1}_{kl,v,s,t} \left(\overline{y^{aux1}_{kl,v}}\right), \\ y^{aux2}_{v,s,t} &= \sum_{kl=1}^{KL} \hbar^{a2}_{kl,v,s,t} \left(\overline{y^{aux2}_{kl,v}}\right) \forall v, s, t \end{aligned} \tag{C.5}$$

$$\begin{aligned} &\sum_{kl=1}^{KL} \hbar^{a1}_{kl,v,s,t} = 1, \sum_{kl=1}^{KL} \hbar^{a2}_{kl,v,s,t} = 1 \forall v, s, t \\ &\hbar^{a1}_{kl,v,s,t} > 0, \hbar^{a2}_{kl,v,s,t} > 0 \end{aligned} \tag{C.6}$$

$$dg^{Lin}_{v,s,t} = FY^{aux1}_{v,s,t} - FY^{aux2}_{v,s,t} \forall v, s, t \tag{C.7}$$

Appendix D. Robust optimization

Consider the following general robust optimization problem:

$$\min_{x} \max_{\Phi} z = c_1 x + c_2 y \tag{D.1}$$

$$x + y = b \; ; \lambda \tag{D.2}$$

$$0 \le x \le \overline{x} \; ; \underline{\mu_1}, \overline{\mu_1} \tag{D.3}$$

$$0 \le y \le \overline{y} \; ; \underline{\mu_2}, \overline{\mu_2} \tag{D.4}$$

Eq. (D.1) expresses the objective function of the problem. The goal of the problem is to find the worst case of the uncertainty variable by the robust optimization method. Where c_1 and c_2 represent the cost parameters and z the objective function of the problem. Moreover, x is a positive decision variable and y is a positive random variable. Eq. (D.2) models the equality equations and Eq. (D.3)–(D.4) express the inequality equations. Where $\overline{x}$ and $\overline{y}$ represent the upper limit of positive decision and positive random variables, respectively. Particularly, the variables $\overline{\mu_{1,2}}, \underline{\mu_{1,2}}$ express the dual inequality equations and the variable λ represents the dual equality equations. We assume that the output of the random variable is volatile within the interval $\left[y^0 - \overline{\Delta y}, y^0 + \overline{\Delta y}\right]$. After adopting the uncertainty parameter, the uncertainty set Φ is described as follows.

$$\Phi := \left\{ \frac{\Delta y}{\overline{\Delta y}} \le \Gamma \quad , \quad \overline{y} = y^0 + \Delta y \right\} \tag{D.5}$$

Where Δy models the difference between the actual value and the predicted value of the uncertainty parameter, and $\overline{\Delta y}$ shows the maximum difference between the actual value and the predicted value of the random variable. Furthermore, the variable y^0 expresses the predicted value of the uncertainty parameter and $\overline{y}$ sets the maximum bounded value of the random variable.

$$
\begin{aligned}
Max \sum_{t} \left[\begin{array}{l}
-\sum_{g} \overline{P^{G}_{g,t}\mu^{1}_{g,t}} - \sum_{g}\sum_{m} \overline{\rho_{g,m}}\overline{\mu^{2}_{g,m,t}} + \underline{p^{Dsc}_{t}}\mu^{7}_{t} - \overline{p^{Dsc}_{t}}\mu^{7}_{t} - \sum_{w} \overline{P^{WT}_{w,t}}\overline{\mu^{8}_{w,t}} + \sum_{d\in A^{d}_{b}} P_{d,t}\lambda^{WEM}_{b,t} \\
-\sum_{b,b'\in Tr} \underline{\upsilon_{b,b',t}}\overline{C_{b,b',t}} - \sum_{b,b'\in Tr} \overline{\upsilon_{b,b',t}}\overline{C_{b,b',t}} - \sum_{b} \pi(\overline{\xi_{b,t}} + \underline{\xi_{b,t}}) - \sum_{g} RU_{g}\mu^{3}_{g,t}|_{t>1} \\
-\sum_{g} (RU_{g} + P^{G}_{g,ini})\mu^{4}_{g,t}|_{t=1} - \sum_{g} RD_{g}\mu^{5}_{g,t}|_{t>1} - \sum_{g} (RD_{g} - P^{G}_{g,ini})\mu^{6}_{g,t}|_{t=1}
\end{array} \right] \\
= Min \sum_{t}\sum_{g}\sum_{m} C^{G}_{g,m}\rho^{G}_{g,m,t} - \sum_{t} C^{Dsc}_{t}p^{Dsc}_{t}
\end{aligned}
\tag{B.1}
$$

Box I.

$$
\begin{aligned}
&\sum_{t} C^{Dsc}_{t}p^{Dsc}_{t} = \sum_{t}\sum_{g}\sum_{m} C^{G}_{g,m}\rho^{G}_{g,m,t} \\
&-\sum_{t} \left[\begin{array}{l}
-\sum_{g} \overline{P^{G}_{g,t}\mu^{1}_{g,t}} - \sum_{g}\sum_{m} \overline{\rho_{g,m}}\overline{\mu^{2}_{g,m,t}} + \underline{p^{Dsc}_{t}}\mu^{7}_{t} - \overline{p^{Dsc}_{t}}\mu^{7}_{t} - \sum_{w} \overline{P^{WT}_{w,t}}\overline{\mu^{8}_{w,t}} + \sum_{d\in A^{d}_{b}} P_{d,t}\lambda^{WEM}_{b,t} \\
-\sum_{b,b'\in Tr} \underline{\upsilon_{b,b',t}}\overline{C_{b,b',t}} - \sum_{b,b'\in Tr} \overline{\upsilon_{b,b',t}}\overline{C_{b,b',t}} - \sum_{b} \pi(\overline{\xi_{b,t}} + \underline{\xi_{b,t}}) - \sum_{g} RU_{g}\mu^{3}_{g,t}|_{t>1} \\
-\sum_{g} (RU_{g} + P^{G}_{g,ini})\mu^{4}_{g,t}|_{t=1} - \sum_{g} RD_{g}\mu^{5}_{g,t}|_{t>1} - \sum_{g} (RD_{g} - P^{G}_{g,ini})\mu^{6}_{g,t}|_{t=1}
\end{array} \right]
\end{aligned}
\tag{B.6}
$$

$$
\begin{aligned}
&\sum_{b,t} p^{Dsc}_{t}\lambda^{WEM}_{b,t} = \sum_{t}\sum_{g}\sum_{m} C^{G}_{g,m}\rho^{G}_{g,m,t} \\
&-\sum_{t} \left[\begin{array}{l}
-\sum_{b,b'\in Tr} \underline{\upsilon_{b,b',t}}\overline{C_{b,b',t}} - \sum_{b,b'\in Tr} \overline{\upsilon_{b,b',t}}\overline{C_{b,b',t}} - \sum_{b} \pi(\overline{\xi_{b,t}} + \underline{\xi_{b,t}}) - \sum_{g} RU_{g}\mu^{3}_{g,t}|_{t>1} \\
-\sum_{g} (RU_{g} + P^{G}_{g,ini})\mu^{4}_{g,t}|_{t=1} - \sum_{g} RD_{g}\mu^{5}_{g,t}|_{t>1} - \sum_{g} (RD_{g} - P^{G}_{g,ini})\mu^{6}_{g,t}|_{t=1} \\
-\sum_{g} \overline{P^{G}_{g,t}\mu^{1}_{g,t}} - \sum_{g}\sum_{m} \overline{\rho_{g,m}}\overline{\mu^{2}_{g,m,t}} - \sum_{w} \overline{P^{WT}_{w,t}}\overline{\mu^{8}_{w,t}} + \sum_{d\in A^{d}_{b}} P_{d,t}\lambda^{WEM}_{b,t}
\end{array} \right]
\end{aligned}
\tag{B.7}
$$

Box II.

Solving robust problems Eq. (D.1)–(D.5) cannot be feasible normally by using commercial solvers (due to min.max). For this purpose, using the duality theory, we convert the min.max problem into a min.min problem as proved in [56,57]. Finally, after solving the following problem, the robust solution of problem Eq. (D.1)–(D.5) is obtained as following exact equations.

$$\min_{x} z = \overline{x\mu_1} + \overline{y\mu_2} + b\lambda \tag{D.6}$$

$$\overline{\mu_1} + \lambda \geq c_1 \tag{D.7}$$

$$\overline{\mu_2} + \lambda \geq c_2 \tag{D.8}$$

$$\begin{aligned} &\overline{\mu_1}, \overline{\mu_2} \geq 0 \\ &\lambda \in \ free\ variable \end{aligned} \tag{D.9}$$

References

[1] Milošević ND, Popović ŽN, Kovački NV. A multi-period multi-criteria replacement and rejuvenation planning of underground cables in urban distribution networks. Int J Electr Power Energy Syst 2023;149:109018.

[2] Li Y, Wei X, Lin J, Niu G. A robust fault location method for active distribution network based on self-adaptive switching function. Int J Electr Power Energy Syst 2023;148:109007.

[3] Esmaeili M, Shafie-khah M, Catalao JP. A system dynamics approach to study the long-term interaction of the natural gas market and electricity market comprising high penetration of renewable energy resources. Int J Electr Power Energy Syst 2022;139:108021.

[4] IRENA. Renewable energy policies in a time of transition. Int J Prod Res 2018;53(9).

[5] Navas-Anguita Z, García-Gusano D, Iribarren D. A review of techno-economic data for road transportation fuels. Renew Sustain Energy Rev 2019;112(April):11–26. http://dx.doi.org/10.1016/j.rser.2019.05.041.

[6] IRENA. IRENA (2019) global energy transformation: A roadmap to 2050. 2019.

[7] Nasiri N, Zeynali S, Ravadanegh SN, Kubler S. Economic-environmental convex network-constrained decision-making for integrated multi-energy distribution systems under electrified transportation fleets. J Clean Prod 2022;379:134582.

[8] Patel M, Roy S, Roskilly AP, Smallbone A. The techno-economics potential of hydrogen interconnectors for electrical energy transmission and storage. J Clean Prod 2022;335:130045.

[9] Parlikar A, Schott M, Godse K, Kucevic D, Jossen A, Hesse H. High-power electric vehicle charging: Low-carbon grid integration pathways with stationary lithium-ion battery systems and renewable generation. Appl Energy 2023;333:120541.

[10] Ullah Z, Wang S, Wu G, Hasanien HM, Rehman AU, Turky RA, et al. Optimal scheduling and techno-economic analysis of electric vehicles by implementing solar-based grid-tied charging station. Energy 2023;267:126560.

[11] Mohammad A, Zamora R, Lie TT. Energy management for EV participation in local energy markets. In: 2022 IEEE transportation electrification conference & expo. ITEC, IEEE; 2022, p. 1327–31.

[12] de la Torre S, Aguado J, Sauma E. Optimal scheduling of ancillary services provided by an electric vehicle aggregator. Energy 2023;265:126147.

[13] Vijayan V, Mohapatra A, Singh S, Dewangan CL. An efficient modular optimization scheme for unbalanced active distribution networks with uncertain EV and PV penetrations. IEEE Trans Smart Grid 2023.

[14] Shi X, Xu Y, Guo Q, Sun H. Optimal dispatch based on Aggregated Operation Region of EV considering spatio-temporal distribution. IEEE Trans Sustain Energy 2021;13(2):715–31.

[15] Gao X, Chan KW, Xia S, Zhang X, Zhang K, Zhou J. A multiagent competitive bidding strategy in a pool-based electricity market with price-maker participants of WPPs and EV aggregators. IEEE Trans Ind Inform 2021;17(11):7256–68.

[16] Sangswang A, Konghirun M. Optimal strategies in home energy management system integrating solar power, energy storage, and vehicle-to-grid for grid

support and energy efficiency. IEEE Trans Ind Appl 2020-09-01;56(5):5716–28. http://dx.doi.org/10.1109/TIA.2020.2991652.
[17] Das S, Acharjee P, Bhattacharya A. Charging scheduling of electric vehicle incorporating grid-to-vehicle and vehicle-to-grid technology considering in smart grid. IEEE Trans Ind Appl 2021-03-01;57(2):1688–702. http://dx.doi.org/10.1109/TIA.2020.3041808.
[18] Patnam BSK, Pindoriya NM. DLMP calculation and congestion minimization with EV aggregator loading in a distribution network using bilevel program. IEEE Syst J 2020;1–12. http://dx.doi.org/10.1109/jsyst.2020.2997189.
[19] Deb S, Goswami AK, Harsh P, Sahoo JP, Chetri RL, Roy R, et al. Charging coordination of plug-in electric vehicle for congestion management in distribution system integrated with renewable energy sources. IEEE Trans Ind Appl 2020;56(5):5452–62. http://dx.doi.org/10.1109/TIA.2020.3010897.
[20] Li Y, Han M, Yang Z, Li G. Coordinating flexible demand response and renewable uncertainties for scheduling of community integrated energy systems with an electric vehicle charging station: A bi-level approach. IEEE Trans Sustain Energy 2021. http://dx.doi.org/10.1109/TSTE.2021.3090463.
[21] Liu W, Chen S, Hou Y, Yang Z. Optimal reserve management of electric vehicle aggregator: Discrete bilevel optimization model and exact algorithm. IEEE Trans Smart Grid 2021;12(5):4003–15. http://dx.doi.org/10.1109/TSG.2021.3075710.
[22] Hajebrahimi A, Kamwa I, Abdelaziz MMA, Moeini A. Scenario-wise distributionally robust optimization for collaborative intermittent resources and electric vehicle aggregator bidding strategy. IEEE Trans Power Syst 2020;35(5):3706–18. http://dx.doi.org/10.1109/TPWRS.2020.2985572.
[23] Li Y, Ni Z, Zhao T, Yu M, Liu Y, Wu L, et al. Coordinated scheduling for improving uncertain wind power adsorption in electric vehicles - wind integrated power systems by multiobjective optimization approach. IEEE Trans Ind Appl 2020;56(3):2238–50. http://dx.doi.org/10.1109/TIA.2020.2976909.
[24] Sharma S, Jain P. Risk-averse integrated DR and dynamic V2G scheduling of parking lot operator for enhanced market efficiency. Energy 2023;275:127428.
[25] Najafi A, Jasiński M, Leonowicz Z. A hybrid distributed framework for optimal coordination of electric vehicle aggregators problem. Energy 2022;249:123674.
[26] Zare M, Chabok H, Niknam T, Azizipanah-Abarghooee R. Smart coordinated management of distribution networks with high penetration of PEVs using FLC. IET Gener, Transm Distribution 2020;14(3):476–85.
[27] Mobaraki AH, Salyani P, Safari A, Quteishat A, Younis MA. A hybrid robust-stochastic optimization model for planned outage based day-ahead scheduling of a plug-in electric vehicles parking lot. Sustain Energy Technol Assess 2022;54:102831.
[28] Sheikhahmadi P, Bahramara S, Mazza A, Chicco G, Catalão JP. Bi-level optimization model for the coordination between transmission and distribution systems interacting with local energy markets. Int J Electr Power Energy Syst 2021;124:106392. http://dx.doi.org/10.1016/j.ijepes.2020.106392.
[29] Mohiti M, Monsef H, Anvari-moghaddam A, Guerrero J, Lesani H. A decentralized robust model for optimal operation of distribution companies with private microgrids. Int J Electr Power Energy Syst 2019;106:105–23. http://dx.doi.org/10.1016/J.IJEPES.2018.09.031.
[30] Hu B, Gong Y, Chung C, Noble B, Poelzer G. Price-maker bidding and offering strategies for networked microgrids in day-ahead electricity markets. IEEE Trans Smart Grid 2021;1. http://dx.doi.org/10.1109/TSG.2021.3109111.
[31] Zhang C, Wang Q, Wang J, Korpås M, Pinson P, Østergaard J, et al. Trading strategies for distribution company with stochastic distributed energy resources. Appl Energy 2016;177:625–35.
[32] Xia Y, Xu Q, Tao S, Du P, Ding Y, Fang J. Preserving operation privacy of peer-to-peer energy transaction based on enhanced benders decomposition considering uncertainty of renewable energy generations. Energy 2022;250:123567.
[33] Xia Y, Xu Q, Tao S, Du P, Ding Y, Fang J. Preserving operation privacy of peer-to-peer energy transaction based on enhanced benders decomposition considering uncertainty of renewable energy generations. Energy 2022;250:123567.
[34] Karimi H, Jadid S. Modeling of transactive energy in multi-microgrid systems by hybrid of competitive-cooperative games. Electr Power Syst Res 2021;201:107546.
[35] Nasiri N, Zeynali S, Ravadanegh SN, Kubler S. Moment-based distributionally robust peer-to-peer transactive energy trading framework between networked microgrids, smart parking lots and electricity distribution network. IEEE Trans Smart Grid 2023.
[36] Nasiri N, Zeynali S, Ravadanegh SN. A tactical transactive energy scheduling for the electric vehicle-integrated networked microgrids. Sustainable Cities Soc 2022;83:103943.
[37] Zeynali S, Nasiri N, Ravadanegh SN, Marzband M. The role of smart electric vehicle charging in optimal decision-making of the active distribution network. In: Electric vehicle integration via smart charging: technology, standards, implementation, and applications. Springer; 2022, p. 201–22.
[38] Nasiri N, Zeynali S, Ravadanegh SN, Kubler S. Economic-environmental convex network-constrained decision-making for integrated multi-energy distribution systems under electrified transportation fleets. J Clean Prod 2022;379:134582.
[39] Cao Y, Li D, Zhang Y, Tang Q, Khodaei A, Zhang H, et al. Optimal energy management for multi-microgrid under a transactive energy framework with distributionally robust optimization. IEEE Trans Smart Grid 2021;13(1):599–612.
[40] Nasiri N, Zeynali S, Ravadanegh SN, Marzband M. A hybrid robust-stochastic approach for strategic scheduling of a multi-energy system as a price-maker player in day-ahead wholesale market. Energy 2021;235:121398. http://dx.doi.org/10.1016/J.ENERGY.2021.121398.
[41] Zeynali S, Nasiri N, Marzband M, Ravadanegh SN. A hybrid robust-stochastic framework for strategic scheduling of integrated wind farm and plug-in hybrid electric vehicle fleets. Appl Energy 2021;300:117432. http://dx.doi.org/10.1016/J.APENERGY.2021.117432.
[42] Xu B, Zhao J, Zheng T, Litvinov E, Kirschen DS. Factoring the cycle aging cost of batteries participating in electricity markets. IEEE Trans Power Syst 2018;33(2):2248–59. http://dx.doi.org/10.1109/TPWRS.2017.2733339.
[43] Bisschop J. AIMMS optimization modeling. 2006.
[44] Bahramara S, Sheikhahmadi P, Mazza A, Chicco G, Shafie-Khah M, Catalão JP. A risk-based decision framework for the distribution company in mutual interaction with the wholesale day-ahead market and microgrids. IEEE Trans Ind Inf 2020;16(2):764–78. http://dx.doi.org/10.1109/TII.2019.2921790.
[45] Xue Y, Shahidehpour M, Pan Z, Wang B, Zhou Q, Guo Q, et al. Reconfiguration of district heating network for operational flexibility enhancement in power system unit commitment. IEEE Trans Sustain Energy 2021;12(2):1161–73. http://dx.doi.org/10.1109/TSTE.2020.3036887.
[46] Sheikhahmadi P, Bahramara S, Mazza A, Chicco G, Catalão JP. Bi-level optimization model for the coordination between transmission and distribution systems interacting with local energy markets. Int J Electr Power Energy Syst 2021;124:106392.
[47] Conejo AJ, Carrión M, Morales JM. Decision making under uncertainty in electricity markets. International series in operations research & management science, vol. 153, Boston, MA: Springer US; 2010, http://dx.doi.org/10.1007/978-1-4419-7421-1.
[48] Yan M, Shahidehpour M, Alabdulwahab A, Abusorrah A, Gurung N, Zheng H, et al. Blockchain for transacting energy and carbon allowance in networked microgrids. IEEE Trans Smart Grid 2021;1. http://dx.doi.org/10.1109/TSG.2021.3109103.
[49] Nikmehr N, Zhang P, Bragin M. Quantum distributed unit commitment. IEEE Trans Power Syst 2022.
[50] National household travel survey: URL https://nhts.ornl.gov/.
[51] Zeynali S, Rostami N, Feyzi M. Multi-objective optimal short-term planning of renewable distributed generations and capacitor banks in power system considering different uncertainties including plug-in electric vehicles. Int J Electr Power Energy Syst 2020;119:105885.
[52] Data available at: URL http://motor.ece.iit.edu/data.
[53] National household travel survey, URL https://nhts.ornl.gov/.
[54] Data repository: URL https://uniluxembourg-my.sharepoint.com/:f:/g/personal/saeid_zeinali_uni_lu/ElUe5JPZi31Lkio3lhTwVBkBefQrQXQljcaj7AiNtoarxQ?e=IO4au9.
[55] Fazlalipour P, Ehsan M, Mohammadi-Ivatloo B. Risk-aware stochastic bidding strategy of renewable micro-grids in day-ahead and real-time markets. Energy 2019;171:689–700.
[56] Apostolopoulou D, De Greve Z, McCulloch M. Robust optimization for hydroelectric system operation under uncertainty. IEEE Trans Power Syst 2018;33(3):3337–48.
[57] Bertsimas D, Sim M. Robust discrete optimization and network flows. Math Program 2003;98(1):49–71.